Research Square

Preprints are preliminary reports that have not undergone peer review.
They should not be considered conclusive, used to inform clinical practice,
or referenced by the media as validated information.

Diacylglyceryl-N,N,N-trimethylhomoserine-dependent Lipid Remodeling in a Green Alga, Chlorella Kessleri

Yutaro Oishi
School of Life Sciences, Tokyo University of Pharmacy and Life Sciences
Rie Otaki
School of Life Sciences, Tokyo University of Pharmacy and Life Sciences
Yukari Iijima
School of Life Sciences, Tokyo University of Pharmacy and Life Sciences
Eri Kumagai
School of Life Sciences, Tokyo University of Pharmacy and Life Sciences
Motohide Aoki
School of Life Sciences, Tokyo University of Pharmacy and Life Sciences
Mikio Tsuzuki
School of Life Sciences, Tokyo University of Pharmacy and Life Sciences
Shoko Fujiwara
School of Life Sciences, Tokyo University of Pharmacy and Life Sciences
Norihiro Sato (nsato@ls.toyaku.ac.jp)
School of Life Sciences, Tokyo University of Pharmacy and Life Sciences

Article

Keywords: betaine lipid, BTA1, Chlorella kessleri, diacylglyceryl-N,N,N-trimethylhomoserine, extraplastid lipids, lipid remodeling, phosphatidylcholine, phosphatidylethanolamine, Pi-recycling, phospholipase C

Posted Date: June 9th, 2021

DOI: https://doi.org/10.21203/rs.3.rs-558352/v1

License: This work is licensed under a Creative Commons Attribution 4.0 International License.
Read Full License

Version of Record: A version of this preprint was published at Communications Biology on January 11th, 2022. See the published version at https://doi.org/10.1038/s42003-021-02927-z.

Title page

Title

Diacylglyceryl-*N*,*N*,*N*-trimethylhomoserine-dependent lipid remodeling in a green alga, *Chlorella kessleri*

Authors

Yutaro Oishi, Rie Otaki, Yukari Iijima, Eri Kumagai, Motohide Aoki, Mikio Tsuzuki, Shoko Fujiwara and Norihiro Sato

Affiliation

School of Life Sciences, Tokyo University of Pharmacy and Life Sciences, Horinouchi 1432-1, Hachioji, Tokyo 192-0392, Japan

Corresponding author

Norihiro Sato

e-mail: nsato@ls.toyaku.ac.jp

Abstract: Membrane lipid remodeling contributes to environmental acclimation of plants. In a green lineage, a betaine lipid, diacylglyceryl-*N*,*N*,*N*-trimethylhomoserine (DGTS), is included exclusively among green algae and non-flowering plants. Here we show that, a green alga, *Chlorella kessleri*, reported to exceptionally possess no DGTS, synthesizes it specifically under phosphorus-deficiency conditions through the eukaryotic pathway via the ER. Simultaneously, phosphatidylcholine and phosphatidylethanolamine, which are similar to DGTS in its zwitterionic property, are almost completely degraded to release 18.1% cellular phosphorus, and to provide its diacylglycerol moieties for a part of DGTS synthesis. Above lipid remodeling system that substitutes DGTS for extrachloroplast phospholipids to lower the P-quota operates through expression induction of the gene for BTA1 that is functionally identified as responsible for DGTS synthesis, and those for phospholipid breakdown. Investigation of this lipid remodeling is necessary in a wide range of lower green plants for a comprehensive understanding of their phosphorus-deficiency acclimation strategies.

Key words: betaine lipid, *BTA1*, *Chlorella kessleri*, diacylglyceryl-*N*,*N*,*N*-trimethylhomoserine, extraplastid lipids, lipid remodeling, phosphatidylcholine, phosphatidylethanolamine, Pi-recycling, phospholipase C.

Introduction

Polar lipids that form lipid bilayers are the foundation for the construction of membranes, where membrane proteins are embedded to contribute to the functionality of the membranes. Information has accumulated over two decades on the remodeling of the membrane lipids crucial for the acclimation to some environmental stresses in photosynthetic organisms or for the compensation of their mutational loss of some polar lipid[1,2]. This lipid remodeling includes phosphorus (P)-limitation stress induced replacement of one anionic lipid, phosphatidylglycerol (PG), with another anionic and non-P lipid, sulfoquinovosyl diacylglycerol (SQDG), in the membranes of plant chloroplasts and in those of some bacteria including the postulated ancestor of chloroplasts, cyanobacteria. The replacement of PG by SQDG is regarded to maintain the charge balance of photosynthetic membranes at a certain level for the proper performance of photosynthesis[2]. Meanwhile, in seed plants, in particular, in their roots and shoots, P-limitation stress also induces a distinct lipid remodeling that substitutes another non-P lipid, digalactosyl diacylglycerol (DGDG), for phosphatidylcholine (PC) in extraplastid membranes[1].

54 Diacylglyceryl-*N*,*N*,*N*-trimethylhomoserine (DGTS), which is one of membrane lipids,
55 possesses both a positively charged trimethylammonium group and a negatively charged
56 carboxyl one. This non-P betaine lipid is therefore categorized as a zwitterionic lipid[3].
57 DGTS is prevalently distributed in evolutionarily lower photosynthetic organisms in a
58 green lineage, including green algae and non-flowering plants such as mosses and ferns[4-
59 6]. Since no DGTS-containing seed plants have been found, it seems that DGTS plays
60 some role specific in lower green plants. DGTS is similar to another zwitterionic lipid,
61 phosphatidylcholine (PC), with respect to chemical and biophysical properties[7]. It is
62 generally accepted that, in green plants including lower ones, PC is localized mainly at
63 extraplastid membranes, as observed in seed plants[8]. Meanwhile, information on the
64 subcellular localization of DGTS is restricted to some green algal species, including, e.g.,
65 its occurrence in plasma membranes in a green alga, *Dunariella. salina*[9,10]. In this context,
66 it is of note that the DGTS content tended to be high in species that possess a low content
67 of PC (Fig.1a, b), which would be interpreted as reflecting functional substitution of
68 DGTS for PC in extrachloroplast membranes[6].
69 Concerning green algae, *Dunaliella* and *Chlamydomonas* species that belong to the
70 Chlorophyceae possess DGTS as one of the major lipids that represents as high as 8.4 to
71 24.3 mol% of total polar lipids, the PC content being low (Fig. 1)[10-14]. In Particular,

72 *Chlamydomonas reinhardtii* and *Chlamydomonas moewusii* are extreme in exclusively
73 possessing DGTS with no PC. In contrast, DGTS was lower in quantity than PC in the
74 green algal species of the Treboxiophyceae, as in *Parietochloris incisa* (Fig. 1)[15]. This
75 tendency was more obvious in *Chlorella* species in particular: DGTS amounted to only
76 1.3% in *Chlorella fusca*, and, above all, it was absent in *Chlorella kessleri* (*Parachlorella*
77 *kessleri* previously known as *C. vulgaris*) and *Chlorella pyreniodosa* with high contents
78 of PC (Fig. 1) [6,16-18].

79 DGTS was observed in other species than lower green plants, although within
80 taxonomically narrow ranges. Several species including the secondary endosymbiotic
81 algae of a red lineage, *Nannochloropsis oceanica*, an anoxygenic photosynthetic
82 bacterium, *Rhodobacter sphaeroides*, and a fungus, *Flammulina velutipes*, were shown
83 to remodel lipids by substituting DGTS for PC upon P-limitation stress[19-21]. Moreover, a
84 DGTS-loss mutation caused cells to be repressed as to acclimating growth under P-
85 limited conditions in *N. oceanica*[20]. To our knowledge, however, information on lipid
86 remodeling is scarce in lower green plants under P-limited conditions, despite its potential
87 involvement in their mechanism of acclimation to the P-stress.

88 *C. kessleri* is industrially attractive because of its ability to synthesize triacylglycerol
89 (TG) at high levels[22-24]. We previously reported that the membrane lipid metabolism in

90 *C. kessleri* is similar to that in a seed plant, *Arabidopsis thaliana*, rather than to in another
91 green alga, *C. reinhardtii*. First, in *C. kessleri* as well as in *A. thaliana*, PC is present with
92 DGTS completely absent whereas, in *C. reinhardtii*, DGTS contrarily exists in the
93 absence of PC [25,26]. Second, the lipid synthesis in chloroplast membranes depends on the
94 cooperation of two lipid biosynthetic pathways, i.e., the prokaryotic pathway within
95 chloroplasts and the eukaryotic pathway via the ER in *C. kessleri* like in *A. thaliana*,
96 whereas it proceeds predominantly through the prokaryotic pathway in *C. reinhardtii* [17,25-
97 27]. Intriguingly, during our study on polar lipids of *C. kessleri* under stress conditions for
98 the induction of TG accumulation, an unidentified lipid with a similar Rf value to that of
99 DGTS was found to appear (Supplementary Fig. 1), which indicated the necessity to
100 reevaluate the membrane lipid metabolism in *C. kessleri*.

101 This study investigated lipid remodeling for acclimation to P-starved conditions in *C.*
102 *kessleri*, in view of well-known quantitative increases of DGTS under these P-stress
103 conditions, and regulatory expression patterns of the genes involved in this remodeling.
104 The results were interpreted as showing that *C. kessleri* is endowed with a sophisticated
105 regulatory mechanism to almost completely replace extraplastid phospholipids including
106 PC with DGTS upon necessity, and that this lipid remodeling is responsible for Pi
107 recycling.

Results

P-starvation induced cell growth defect in *C. kessleri.* This study investigated the polar lipid composition under conditions of P-starvation (-P) in *C. kessleri* to reevaluate its lipid metabolim. We first examined the effects of -P on cell growth in *C. kessleri*. As compared with P-repletion (+P) conditions, -P ones had little deleterious effect on cell growth for the first 24 h, however, causing retardation of cell growth for the next 48 h (Fig. 2a). In line, the chlorophyll (Chl) content of the culture increased more slowly under -P conditions than under +P ones (Fig. 2b). The cellular Chl content on an OD_{730}·ml basis therefore remained lower under -P conditions than under +P ones throughout the culturing (Fig. 2c). Meanwhile, the total cellular P content, which had initially been 157.1 nmole/(OD_{730}·ml), drastically decreased to 24.9 nmole/(OD_{730}·ml) in 48 h under -P conditions, relative to a mild reduction to 112.6 nmole/(OD_{730}·ml) under +P conditions (Fig. 2d). Despite the severe shortage of P, the survival ratio was little affected in -P cells (95.1%, c.f., 96.4% in +P cells), which demonstrated proper -P-acclimation of *C. kessleri* cells (Fig. 2e).

P-starvation induced lipid remodeling in *C. kessleri*. We then investigated whether or not the mechanism of *C. kessleri* cells for acclimating to -P stress involves lipid-remodeling. TLC analysis exhibited that the shift of *C. kessleri* cells from +P to -P conditions brought about the appearance of a novel lipid at a substantial level at 24 h, followed by persistent maintenance of the level for the next 48 h (Lipid X, Fig. 3a, b). The novel lipid was subjected to ESI-MS^2 analysis. Its ESI mass spectra showed two protonated positive ions, m/z 737 and 761, and their respective sodium adduct ions, m/z 759 and 783 (Fig. 4a). Meanwhile, DGTS prepared from *C. reinharditii* gave protonated m/z 735 and 737 signals and their sodium adducts, m/z 757and 759 (Fig. 4b). It was of note that the product ion spectrum at m/z 737 for *C. kesssleri* exhibited product ions of m/z 144, 162 and 236, which were common to those of m/z 735 in *C. reinhardtii* (Fig. 4c, d). These results allowed us to identify the novel lipid as DGTS, compatible with the previous report[28]. Accordingly, it was interpreted that the product ions, m/z 456 and 474, and m/z 480 and 498, resulted from the loss of 18:2 and that of 16:0, respectively, in *C. kessleri* (Fig. 4c). Similarly, the product ion spectrum of m/z 761 exhibited three signals (m/z 144, 162 and 236) leading to its identification as DGTS, and two signals for the loss of 18:2 (m/z 480 and 498) (Fig. 4e). These results, together with fatty acid analysis at the

144 *sn*-2 position (see below), clarified that the DGTS molecular species in P-starved *C.*
145 *kessleri* consisted predominantly of *sn*-1 16:0/ *sn*-2 18:2 and *sn*-1 18:2/ *sn*-2 18:2 species.
146 Subsequent quantitative GC analysis of the constituent fatty acids in individual polar
147 lipids showed drastically different lipid compositions between +P and -P cells: PC and
148 phosphatidylethanolamine (PE) amounted to 11.3 and 5.6 mol%, respectively, relative to
149 total polar lipids in +P cells with no DGTS, whereas DGTS accumulated to 21.0 mol%
150 in -P cells with disappearance of PC and PE (Fig. 3c). Another phospholipid, PG,
151 amounted to 12.6 mol% in +P cells, however, it decreased to only 2.3 mol% in -P cells.
152 Besides, -P cells showed a lower content of monogalactosyl diacylglycerol (MGDG)
153 (36.2 mol%, c.f., 43.6 mol% in +P cells) with higher ones of DGDG (24.0 mol%, c.f.,
154 14.9 mol% in +P cells) and SQDG (16.5 mol%, c.f., 12.0 mol% in +P cells). It thus turned
155 out that *C. kessleri*, as well as other lower green plants, can synthesize DGTS, and that
156 this ability is displayed under -P conditions, but not under +P conditions. Besides, typical
157 lipid remodeling at chloroplast membranes occurred in *C. kessleri*, as reported in other
158 photosynthetic organisms, such that PG decreased with a concomitant increase of SQDG,
159 probably to keep the charge of the membranes at a certain level (Fig. 3a-c; Sato, 2004).
160 Based on the Pi content of total cellular fraction and those of individual phospholipids
161 in +P cells, the quantitative proportions of phosphate contents in individual phospholipids

to the total cellular fraction one was estimated to reach 12.1, 6.0, and 13.5% Pi in PC, PE, and PG, respectively (Fig. 3d). Therefore, PC and PE totally accounted for 18.1% and 17.6% of total Pi in +P cells and -P cells, respectively (Fig. 3d).

-P-induced DGTS synthesis via prokaryotic pathway. Individual lipids in +P cells showed their characteristic fatty acid compositions, as previously reported (Fig. 5a-f)[17]. Concerning chloroplast glycolipids, MGDG, in particular, and DGDG contained substantial amounts of unsaturated C_{16} and/or C_{18} acids such as 16:3 and 18:3 (Fig. 5a, b). SQDG had 16:0 and 18:2 as major fatty acids while PG mainly included a sole trans-unsaturated fatty acid, 16:1(3*t*), besides 16:0 and 18:2 (Fig. 5c, d). As to extrachloroplast lipids, PC and PE, mainly contained 16:0 and 18:2 (Fig. 5e, f). Meanwhile, MGDG in -P cells, as compared with that in +P ones, contained 18:3 and 16:3 more abundantly at the expense of 18:2 and 16:2, with DGDG and SQDG respectively displaying only small effects of -P, if any, on their fatty acid compositions. PG was characteristic to demonstrate a higher content of 16:1(3t) in -P cells than in +P ones, at the expense of 16:0. Intriguingly, the fatty acid composition in DGTS in -P cells was almost the same as those in PC and PE in +P cells, such that 16:0 and 18:2 amounted to 20-30 and 55 mol%, respectively (Fig. 5e-g).

Membrane lipids are synthesized through the prokaryotic and eukaryotic pathways in *C. kessleri* as well as in *A. thaliana*[17,26]. The prokaryotic and eukaryotic pathways are responsible for the synthesis of polar glycerolipids with C_{16} and C_{18} acids esterified, respectively, at the *sn*-2 position of the glycerol backbone. DGTS was then analyzed as to the fatty acid composition at the *sn*-2 position to estimate the proportions of prokaryotic and eukaryotic lipids (Fig. 5h). The results indicated that the *sn*-2 position was occupied almost exclusively by C_{18} acids, and strongly implied that DGTS, similar to PC and PE, was synthesized almost exclusively through the eukaryotic pathway.

The metabolic mechanism of -P-induced DGTS accumulation in *C. kessleri*. The structural similarity of DG moieties of DGTS, and PC and PE raised the possibility that PC and PE release their fatty acid and/or DG moieties upon their degradation for DGTS synthesis. Quantitative changes in these three zwitterionic lipids were then chased for a shorter term within 24 h after the shift of +P cells to -P conditions (Fig. 6a, b). DGTS accumulation steeply increased from an initial zero level in 24 h of -P stress, both PC and PE concomitantly steadily decreasing to less than 10% the initial levels at 24 h in the cells when estimated per on the basis of OD_{730}·ml (Fig. 6a). It was of note that the accumulated content of DGTS was close to the total content of PC and PE decreases, which was

198 compatible with the results in Fig. 3c (48 h). However, the increased level of DGTS at 24
199 h was more than ca. 5-fold higher than the sum of the initial levels of PC and PE when
200 estimated per ml culture (Fig. 6b). These results raised the possibility that fatty acids or
201 DG moieties for DGTS synthesis were supplied partially by preexisting PC and PE
202 through their degradation, and more abundantly by other metabolic sources like de novo
203 fatty acid synthesis.

204 The effects of metabolic inhibitors on -P-induced DGTS accumulation were
205 investigated to gain an insight into the metabolic mechanism of lipid remodeling (Fig.
206 6c). Cycloheximide, an inhibitor of 80S ribosomes, almost completely repressed DGTS
207 accumulation under -P conditions, whereas chloramphenicol, an inhibitor of 70S
208 ribosomes in chloroplasts or mitochondria, caused only low repression of DGTS
209 accumulation by 24.1%. These results implied that -P-induced DGTS accumulation
210 depended almost completely on the synthesis of nuclear-genome encoded proteins, and
211 not so greatly on that of chloroplast- or mitochondria-genome encoded proteins.
212 Intriguingly, cerulenin, an inhibitor of β-ketoacyl-ACP synthase of fatty acid synthase,
213 inhibited DGTS accumulation by 27.3%, which inferred involvement not only of de novo
214 synthesized fatty acids, but also of fatty acids originating from pre-existing lipids, in the
215 DGTS accumulation, as was above suggested. Meanwhile, DGTS accumulation was

repressed by 89.0% on application of 3-(3,4-dichlorophenyl)-1,1-dimethylurea (DCMU), an inhibitor of photosynthesis, or through a shift of the cells to dark conditions, which suggested the dependence of DGTS accumulation almost completely on photosynthesis.

Identification of the gene for DGTS synthesis in *C. kessleri*. We then searched for the gene for DGTS synthesis in the genomic DNA sequence of *C. kessleri* with the use of the protein product of the *C. reinhartii BTA1* gene (CrBTA1) as a query[29]. We found a DNA region that could encode a protein highly homologous to CrBTA1. The cDNA covering this region was synthesized through 5'- and 3'-RACE PCR with the use of total RNA isolated from *C. kessleri* cells starved of P, as the template. The primers for 5'- and 3'-RACE PCR were set such that a partially overlapping DNA regions were generated, thereby 1.5-kbp and 2.0-kbp DNA fragments being generated. Subsequent determination of the obtained PCR products revealed that the full-length DNA was 2073 bp long, which was postulated to encode a 78.8 kDa protein that comprised 631 amino acid residues. This protein was composed of two domains that were homologous to the bacterial BtaB (S-adenosylmethionine-diacylgycerolhomoserine-N-methlytransferase) and BtaA (S-adenosylmethionine-diacylglycerol 3-amino-3-carboxypropyl transferase) proteins at the N- and C-terminal halves, respectively (Fig. 7a). This homolog of *C. kessleri* was thus

234 characterized as type B like *C. reinhardtii* BTA1 (CrBTA1), distinct from type A
235 composed of N-terminal BtaA- and C-terminal BtaB-like domains, and showed 62.1%
236 identity in amino acid sequence with CrBTA1. Furthermore, the consensus sequence, VD,
237 for the binding of S-adenosyl methionine as the substrate was conserved in both the BtaA-
238 and BtaB-like domains (Fig. 7a)[29]. The coding region of the full-length cDNA was
239 divided into 18 exons by 19 introns in the genome (Fig.7b). Owing to these sequence
240 characteristics of this protein product, it was strongly suggested that this homologous
241 gene encodes BTA1 for DGTS synthesis. We then functionally characterized this gene
242 through overexpression of its cDNA in *E. coli* cells that intrinsically lack DGTS. Upon
243 induction of the corresponding protein, a novel lipid was found to appear in *E. coli* cells
244 (Fig. 7c), which was thereafter identified as DGTS (Fig. 7d, e). These results proved that
245 the homologous gene of *C. kesleri* encodes the BTA1 protein, and thus the gene was
246 designated as *CkBTA1*.

247 Molecular phylogenetic analysis indicated that the BtaA domain of CkBAT1 is closely
248 related to the counterparts of green algae that belong to the Trebouxiophyceae and
249 Chlorophyceae, and also to those of non-flowering plants, ferns and mosses (Fig. 8a).
250 However, the clade of green algae including *C. kessleri* was far away from the clade of
251 another green algal group, the Prasinophyceae, and secondary endosymbiotic algae, but

252 rather was close to the clade of fungi. A similar trend was observed for the BtaB domain
253 (Fig. 8b). Meanwhile, bacterial BtaA and BtaB showed single clades, respectively.
254
255 **Transcriptional upregulation of the genes for -P-induced lipid remodeling.** Semi-
256 quantitative analysis of mRNA levels as to individual genes was then performed (Fig. 9).
257 *CkBTA1* mRNA level was very low under +P conditions, consistent with the complete
258 absence of DGTS, and increased under -P conditions with time, in line with DGTS
259 accumulation. Meanwhile, the degradation of PC and PE might be catalyzed by non-
260 specific phospholipase C (NPC) and phospholipase D (PLD)[1]. A search for corresponding
261 genes in the *C. kessleri* genome, with *A. thaliana* orthologs of NPC and PLD genes as
262 queries, led us to find that *C. kessleri* has no homologous genes. Alternatively, *C. kessleri*
263 contained two genes coding for proteins homologous to glycerophosphodiester
264 phosphodiesterase with possible PLC activity in *C. reinhardtii* [30]. The expression of one
265 of these candidate *PLC* genes (Cre03.g203600.t1.2, $PLCc_1$), similar to that of *CkBTA1*,
266 was strictly repressed at the transcript level under +P conditions, and was up-regulated
267 with time after the shift to -P conditions, consistent with the progress of the degradation
268 of PC and PE. Meanwhile, the other candidate gene (Cre16.g683850.t1.3, $PLCc_2$) was
269 little affected in its mRNA level, irrespective of the conditions of P. There was the

possibility that phosphocholine and phosphoethanolamine, which might be the degradation products of PC and PE, respectively, by the PLC activity of *PLCc1*, were subjected to the action of phosphatase for Pi release. In accordance with this idea, the mRNA level of the candidate of phosphatase gene *PLP*[31,32] was markedly up-regulated from an almost undetectable level upon -P stress (Fig. 9). These observations implied that the genes responsible for the lipid remodeling were subjected to up-regulation at least at their transcript levels, which seemed compatible with the dependence of DGTS accumulation on the synthesis of proteins encoded by nuclear genes (Fig. 6c).

Discussion

Taxonomical distribution of DGTS in primary endosymbiotic algae. The presence of DGTS has been reported in many lower green plants, with the rare exceptional observation of no detection of it in *C. kessleri* and *C. pyrenoidosa*. However, this study demonstrated that *C. kessleri* cells are able to synthesize DGTS, and that this ability is displayed under -P conditions, but not under +P ones (Figs. 3, 4 & 6). This -P-stress specific DGTS appearance is the reason why DGTS has never thus far been detected in

288 *C. kessleri* [6,16]. It will be necessary to reevaluate the previously reported absence of DGTS
289 in *C. pyrenoidosa*, which might lead to the novel notion of a general ability of DGTS
290 synthesis in green algae.

291 In contrast to the prevalent distribution of DGTS in green algae, the presence of DGTS
292 has been reported within only a taxonomically limited range in red algae. In a red
293 microalga, *Galdieria sulphuraria*, DGTS was one of the major polar lipids[33], which was
294 intriguing with respect to its synthetic pathway since this alga possesses no *BTA1*
295 homolog in its genome (https://phycocosm.jgi.doe.gov/Galsul1/Galsul1.home.html).
296 However, the presence of DGTS have been ruled out in other red microalgae[34-36].
297 Concerning red macroalgae, the presence of DGTS might have been arguable, because of
298 its detection only in limited species, and, if any, at very low levels[4,34]. The question of red
299 macroalgal DGTS would be settled with the use of the lipidomic technique[37,38]. Overall,
300 the taxonomical distribution of DGTS should be carefully examined from both
301 biochemical and genetical aspects, as shown by this study. The use of -P conditions would
302 be necessary for biochemical detection of DGTS and its identification in case of strict
303 regulation of the responsible gene, as observed in *C. kessleri*.

304

305 **Physiological significance of lipid remodeling in *C. kessleri* cells in response to**

306 **-P stress.** To our knowledge, information on the effects of -P on the DGTS contents in
307 lower green plants is limited to that in *C. reinhardti*. Distinct from non-green
308 photosynthetic and non-photosynthetic organisms known to show -P-induced DGTS
309 increases, *C. reinhardtii* showed little effect of -P on the DGTS content, which might
310 imply that this green alga has adapted to -P-stress in freshwater habitats by losing PC[19-
311 21,39]. Our study therefore demonstrated -P-specific induction of DGTS synthesis in *C.*
312 *kessleri* among lower green plants, as a unique lipid remodeling pattern that accompanies
313 almost complete degradation of PC and PE at extrachloroplast membranes. In vitro assay
314 demonstrated that DGTS was synthesized not in isolated chloroplasts, but in microsomal
315 fractions in *C. reinhardtii* whereas the counterpart of BTA1 is localized at the ER in a
316 fungus, *F. graminearum*[21,40]. It is therefore highly probable that CkBTA1 contributes to
317 DGTS synthesis at extrachlorolast membranes such as ER ones through the eukaryotic
318 pathway (Fig. 5h). Accordingly, DGTS as well as PC and PE would be present mainly at
319 extrachloroplast membranes in *C. kessleri*, as previously reported in other algal species
320 [10]. In this context, it was of note that the relative contents of these two phospholipids, PC
321 and PE, in +P cells were very close to that of DGTS in -P cells (Figs. 3c & 6a). Since
322 DGTS is similar to PC in zwitterionic and biophysical properties, and also to PE in the

323 zwitterionic one to PE[7], we propose that DGTS functionally substitutes for PC and PE in
324 *C. kessleri* at extrachloroplast membranes under -P conditions.

325 Seed plants adopted another lipid remodeling system at extraplastid membranes in
326 roots and shoots to replace phospholipids such as PC with DGDG[1]. The DGDG content
327 increased also in *C. kessleri*, however, by only 1.6-fold in -P cells relative to in +P ones
328 (Fig. 3c; c.f., >8- fold increase of DGDG in roots of *A. thaliana*[41]). This small increase of
329 DGDG might reflect the lipid remodeling at chloroplast membranes, in view of a similarly
330 small increase of the DGDG content by 1.2-fold in -P cells of a cyanobacterium,
331 *Synechocystis* sp. PCC 6803[42]. These results thus prompted us to conclude that *C. kessleri*,
332 quite different from seed plants, utilizes DGTS as a main player in the -P-responsive lipid
333 remodeling at extraplastid membranes.

334 The expression of PLC_{C1} as the PLC candidate was induced under -P conditions,
335 concomitantly with *PLP* mRNA up-regulated. Induced PLC_{C1} and PLP might
336 cooperatively degrade PC and PE to release DG and Pi (Figs. 3 & 9). In line with the
337 possible DG release, the chemical structure of DG moieties as to fatty acids of PC and
338 PE was similar to that of DGTS. Therefore, these observations, together with the partial
339 induction of DGTS synthesis with de novo synthesis of fatty acids being inhibited (Fig.
340 6c), prompted us to propose the involvement of PLC_{C1} in a part of DGTS synthesis

through release of DG (Fig. 6b). The up-regulation of *PLC$_{C1}$* expression was reminiscent of the role of PLC in DG supply through PC degradation in the synthesis of DGTS and DGDG in a bacterium, *Sinorhizobium meliloti*, and *A. thaliana,* respectively, under -P conditions[43,44]. Identification of the actual enzymatic activity of PLC$_{C1}$ awaits a future study.

In view of the Pi content included in PC and PE (18.1% of total cellular Pi), the involvement of PLP in their degradation would enable *C. kessleri* cells to enlarge a Pi-pool under -P conditions, thereby giving a great advantage for -P acclimation. Major phospholipids, i.e., PC, PE, and PG, accounted for 31.6% of total cellular Pi in *C. kessleri*, which was similar to the counterparts occupying 23% of total Pi in the photosynthetic tissues in seed plants (Fig. 3d)[45]. Besides phospholipids, nucleic acids occupy 35% total Pi in photosynthetic tissues of seed plants, with more than 85% of it being attributed to rRNA. Accordingly, major RNases, RNS1 and RNS2, played important roles in rRNA degradation for remobilization of Pi[46]. It will be necessary in the future to investigate other Pi-scavenging systems than DGTS-lipid remodeling in *C. kessleri* as a model green alga, which would lead to a comprehensive understanding of Pi-sequestering systems that is necessary for obtaining the whole picture of the -P-acclimation mechanism in lower green plants.

Evolutionary insight into lipid remodeling in a green lineage. The convincing proof of DGTS occurrence in lower green plants, together with increasing information on their possession of *BTA1* homologs, prompted us to propose that the DGTS synthesis ability appeared in green algae during the evolution of a green lineage. However, the origin of *BTA1* seems different between the Chlorophyceae and Treboxiophyceae, and the Prasinophyceae, as judged from the respective molecular phylogenetic characteristics of the BtaA and BtaB domains, and the fusion order of these two domains in BTA1 proteins (Fig. 8). From the phylogenetic trees of the BtaA and BtaB domains in BTA1, it might be interpreted that, through the evolution of a green lineage, type B BTA1 was first acquired by some ancestral green alga, and thereafter inherited by the Chlorophyceae and Treboxiophyceae, and finally ferns and mosses, however, without its further inheritence to seed plants.

As to the composition of zwitterionic lipids, DGTS and PC, lower green plants possessing type B BTA1 can be grouped into three groups, i.e., those containing DGTS only, both DGTS and PC, and PC only, respectively, under +P conditions. One idea is that the first species originally containing PC acquired the *BTA1* gene, and then evolved to persistently possess both DGTS and PC, as in, e.g., *D. salina*. Later, it seems that green

algae selected one of these two zwitterionic lipids for their membrane construction under +P conditions: some species like *C. reinhardtii* have evolved to contain DGTS only by abandoning PC synthesis with the loss of the PC synthesis genes[39], while other species like *C. kessleri* have chosen PC by repressing the expression of *BTA1*.

It is possible that some ancestral lower green plant like *C. kessleri* lost the *BTA1* gene to evolve into extant seed plants, with the acquisition of the DGDG-utilizing lipid remodeling system. The acquisition of this new remodeling system would have had a beneficial effect on nitrogen (N)-economization, and thus on acclimation to N-limitation stress generally encompassing plant habitats, since DGDG, which unlike DGTS includes no N atom. Simultaneously, complete replacement of DGTS with PC, along with the selection of DGDG-utilizing lipid remodeling, might have merited the evolutionary appearance of extant seed plants, since a variety of their biological processes, such as stress acclimation and plant development, are mediated through PC-related signaling pathways with the actions of phospholipases[47].

Methods

395 **Strain and growth conditions.** *C. kessleri* 11 h was photoautotrophically grown with
396 4-fold diluted Gamborg's B5 (GB5, +P) medium or the -P medium made through
397 replacement of $NaH_2PO_4H_2O$ by equimolar KCl[23.24]. The OD_{730} value and Chl content
398 were measured to monitor cell growth[24]. The cells were precultured in +P medium to an
399 OD_{730} value of ca. 0.5, and then adjusted to an OD_{730} value of 0.2 with +P or -P medium
400 for further growth. The survival ratio of the cells in the culture was examined through 5
401 μM SYTOX-staining (Invitrogen Molecular Probes[48]). When indicated, the culture was
402 supplemented with cycloheximide (8 $\mu g \cdot ml^{-1}$), chloramphenicol (100 $\mu g \cdot ml^{-1}$), cerulenin
403 (10 μM), and DCMU (50 μM) as metabolic inhibitors, or shifted to dark conditions,
404 simultaneously with the commencement of -P culturing.
405
406 **Quantitation of Pi in *C. kessleri* cells.** Cells were harvested from 20 ml culture by
407 centrifugation after washing three times with -P medium, and thereafter disrupted with a
408 Beads Crusher μT-12 (Taitec, Saitama, Japan) in 2 ml of extraction buffer comprising
409 5 mM HEPES-NaOH, pH 7.5, and 10 mM NaCl[24]. To 100 μL of each whole cell extract,
410 2 mL of 15 mM potassium peroxodisulfate and 5 mL of distilled H_2O were added, the
411 resultant solution being subjected to autoclave treatment (121ºC, 30 min) for the release
412 of Pi from P-containing compounds. To 100 μl of the autoclave-treated solution, 300 μL

413 of a 1.22% malachite green G (Wako, Tokyo) solution and 600 μl of distilled H_2O were
414 added, and then the resultant solution was left to stand for 30 min. The Pi content was
415 determined in the marachite-green stained solution through spectroscopic measurement
416 of the absorbance at 639 nm[49].
417
418 **Separation and quantitation of individual polar lipids.** Cells were harvested at the
419 indicated times for the extraction of total lipids, which were then used for separation of
420 individual polar lipids by two-dimensional TLC[50]. A novel lipid found in this study was
421 identified through mass spectrometric analyses. Samples were diluted in IPA/MeOH/H_2O
422 (5:4:1, v/v/v) containing 10 mM ammonium acetate, and then directly infused at 10
423 μL/min flow into a triple quadrupole linear ion trap mass spectrometer (MS) equipped
424 with an electro spray ionization (ESI) source (3200Q with a Trap Turbo V ion source;
425 Sciex, CA). The optimized parameters for DGTS under positive and negative ionization
426 conditions were as follows: Ion spray voltage, 5500 V (positive) and -4500 V (negative);
427 declustering voltage, 100 V (positive) and -55 V (negative); temperature, ambient (both
428 positive and negative). The collision energies for product ion scanning were 60 V
429 (positive) and -45 V (negative). The mass range was scanned m/z 600–900 in the
430 Enhanced Mass Scan (EMS) mode for precursor ions and m/z 50–900 in the Enhanced

Product Ion Scan (EPI) mode for product ions. The mass spectrum data were analyzed with reference to DGTS of *Chlamydomonas reinhardtii* 137c and that of chlorarachniophytes[28]. DGTS from *C. kessleri* was used for the preparation of *sn*-2 monoacyl lysoDGTS through TLC after treatment of it with *Rhizomucor miehei* lipase (Sigma-Aldrich)[17]. Fatty acid methyl esters derived from total lipids, individual polar lipids or *sn*-2 monoacyl lysoDGTS were quantified by capillary GLC based on their constituent fatty acids[17].

Cloning of cDNA for BTA1, determination of its nucleotide sequence, and its expression in *E. coliI.* A blast search was performed with the amino acid sequence of BTA1 of *C. reinhardtii* (CrBTA1) as a query in the genomic DNA database of *C. kessleri* (https://blast.ncbi.nlm.nih.gov/Blast.cgi?PROGRAM=tblastn&PAGE_TYPE=BlastSearch&BLAST_SPEC=Assembly&LINK_LOC=blasttab&ASSEMBLY_NAME=GCA_001598975.1). Sixteen regions that aligned closely on the genome were hit, and therefore, as a whole, were postulated to encode a BTA1 homolog. One of these regions was chosen for primer setting for 5'- and 3'-race PCR with a SMARTer RACE 5'/3' kit (Takara,Tokyo; primer set 1, Supplementary Table 1), the nucleotide sequence of the

448 amplified DNA being determined with a BigDye Terminator v3.1 cycle sequencing kit
449 on a 3500 genetic analyzer (Thermofisher, Tokyo).

450 For heterologous expression of *BTA1* in *E. coli*, the ORF of the *BTA1* cDNA was
451 amplified by PCR with primer set 2 (Supplementary Table 1), and then ligated to a
452 pMAL-c5X vector (New England Biolabs Japan, Tokyo), for generation of the vector
453 designated as pMAL-*BTA1*. The pMAL-*BTA1* or empty pMAL-c5X vector was
454 introduced into NEB express competent *E. coli* cells (New England Biolabs Japan,
455 Tokyo). Transformed cells were subjected to the induction of gene expression with IPTG,
456 and then to SDS-PAGE analysis of total cellular proteins, as described in the
457 manufacture's manual, and to TLC analysis of lipids.

458

459 **Phylogenetic tree.** For phylogenetic analysis, the amino acid sequences of BTA1
460 homologs were searched for in available databases with CrBTA1
461 (CHLREDRAFT_77062), and BtaA (RSP_0856) and BtaB (RSP_0857) of *Rodobacter*
462 *sphaeroides* 2.4.1, as queries. The homolog sequences of CrBTA1 obtained are
463 summarized in Supplementary Table 2. The sequences were aligned after edition
464 including the deletion of lowly conserved regions among these sequences with Geneious
465 9.1.8 (Tomy Digital Biology, Tokyo), and thereafter, the aligned sequences were

466 subjected to phylogenetic analysis with IQ-tree 1.6.12 by the maximum-likelihood
467 method[51].
468
469 **Semi-quantitative PCR analysis.** Total RNA was extracted from *C. kessleri* cells by
470 phenol–chloroform extraction for cDNA synthesis by random-primer based reverse-
471 transcription[24]. Subsequently, the synthesized cDNA was used as a template for semi-
472 quantitative RT-PCR. Specific forward (F) and reverse (R) primer sets 3-6 were designed
473 for the respective genes (Supplementary Table 1), on the basis of the information on
474 above described genomic DNA sequences of *C. kessleri*. The amplified DNA fragments
475 were separated by agarose gel electrophoresis, and then subjected to staining with
476 ethidium bromide to obtain a fluorescent image by photography[52]. The fluorescence
477 intensities of DNA bands for the individual genes were estimated with ImageJ
478 (http://rsbweb.nih.gov/ij/), relative to that for the β-actin gene (*ACT*), as an internal
479 control.
480
481
482 **References**
483

1. Nakamura, Y. Phosphate starvation and membrane lipid remodeling in seed plants. *Prog. Lipid. Res.* **52**, 43-50 (2013).

2. Sato, N. Roles of the acidic lipids sulfoquinovosyl diacylglycerol and phosphatidylglycerol in photosynthesis: their specificity and evolution. *J. Plant Res.* **117**, 495-505 (2004).

3. Brown, A.E. & Elovson, J. Isolation and characterization of a novel lipid, 1(3),2-diacylglyceryl-(3)-O-4'-(N,N,N-trimethyl)homoserine, from *Ochromonas danica*. *Biochem.* **13**, 3476-3482 (1974).

4. Künzler, K. & Eichenberger, W. Betaine lipids and zwitterionic phospholipids in plants and fungi. *Phytochem.* **46**, 883-892 (1997).

5. Sato, N. & Furuya, M. Distribution of diacylglyceryltrimethylhomoserine in selected species of vascular plants. *Phytochem.* **23**, 1625-1627 (1984).

6. Sato, N. & Furuya, M. Distribution of diacylglyceryltrimethylhomoserine and phosphatidylcholine in non-vascular green plants. *Plant Sci.* **33**, 81-85 (1985).

7. Sato, N. & Murata, T. Transition of lipid phase in aqueous dispersions of diacylglyceryltrimethylhomoserine. *Biochim. Biophys. Acta* **1082**, 1006-1017 (1991).

8. Moore, T.S. Phospholipid biosynthesis. *Annu. Rev. Plant Physiol.* **33**, 235–259 (1982).

9. Eichenberger, W. & Gerber, A. Lipids of *Acetabularia mediterranea*. Composition, cellular localization and biosynthesis. In: Stumpf, P..K., Mudd, J.B. & Nes, W.D. (eds.) The Metabolism, Structure, and Function of Plant Lipids. Springer, Boston, MA. (1987).

10. Sheffer, M., Fried, A., Gottlieb, H.E., Tieat, A. & Avron, M. Lipid composition of the plasma-membrane of the halotolerant alga, *Dunaliella salina*. *Biochim. Biophys. Acta* **857**, 165-172 (1986).

11. Arisz, S.A., van Himbergen, J.A.J., Musgrave, A., van den Ende, H. & Munnik, T. Polar lipids of *Chlamydomonas moewusii*. *Phytochem.* **53**, 265-270 (2000).

12. Evans, R.W., Kates, M., Ginzburg, M. & Ginzburg, B.J. Lipid composition of halotorelant algae, *Dunaliella parva* lerche and *Dunaliella tertiolecta*. *Biochim. Biophys. Acta* **712**, 186-195 (1982).

13. Fried, A., Tietz, A., Ben-Amotz, A. & Eichenberger, E. Lipid composition of the halotolerant alga, *Dunaliella bardawil*. *Biochim. Biophys. Acta* **713**, 419-426 (1982).

14. Sato, N. et al. Isolation and characterization of mutants affected in lipid metabolism of *Chlamydomonas reinhardtii*. *Eur. J. Biochem.* **230**, 987-993 (1995).

517 15. Bigogno, C. et al. Lipid and fatty acid composition of the green oleaginous alga
518 *Parietochloris incisa*, the richest plant source of arachidonic acid. *Phytochem.* **60**, 497-
519 503 (2002).
520 16. Eichenberger, W. Distribution of diacylglyceryl-O-4-(N, N, N-trimethyl)homoserine
521 in different algae. *Plant Sci. Lett.* **24**, 91-95 (1982).
522 17. Sato, N., Tsuzuki, M. & Kawaguchi, A. Glycerolipid synthesis in *Chlorella kessleri*
523 11h: II. Effects of the CO_2 concentration during growth. *Biochim. Biophys. Acta* **1633**,
524 35-42 (2003).
525 18. Weber, N., Bergenthal, D., Kokate, C.K. & Mangold, H.K. Biologically active ether
526 lipids: incorporation of long-chain precursors into 1(3),2-diacylglycero-3(1)-O-4'-
527 (N,N,N-trimethyl)homoserines and other lipids of *Chlorella fusca*. *J. Lipid Med.* **1**,
528 37-48 (1989).
529 19. Benning, C., Huang, Z.H. & Gage, D.A. Accumulation of a novel glycolipid and a
530 betaine lipid in cells of *Rhodobacter sphaeroides* grown under phosphate limitation.
531 *Arch. Biochem. Biophys.* **317**, 103-111 (1995).
532 20. Murakami, H., Nobusawa, T., Hori, K., Shimojima, M. & Ohta, H. Betaine lipid
533 crucial for adapting to low temperature and phosphate deficiency in *Nannochloropsis*.
534 *Plant Physiol.* **177**, 181-193 (2018).

21. Zhang, Y. et al. Cellular tracking and gene profiling of *Fusarium graminearum* during maize stalk rot disease development elucidates its strategies in confronting phosphorus limitation in the host apoplast. *Plos Pathog.* **12**, e1005485; 10.1371/journal.ppat.1005485 (2016).

22. Hayashi, T., Otaki, R., Hirai, K., Tsuzuki, M. & Sato, N. Optimization of seawater-based triacylglycerol accumulation in a freshwater green alga, *Chlorella kessleri*, through simultaneous imposition of lowered-temperature and enhanced-light intensity. *Algal Res.* **28**, 100-107 (2017).

23. Hirai, K. et al. Hyperosmosis and its combination with nutrient-limitation are novel environmental stressors for induction of triacylglycerol accumulation in cells of *Chlorella kessleri*. *Sci. Rep.* **6**, 25825; 10.1038/srep25825 (2016).

24. Otaki, R., Oishi, Y., Abe, S., Fujiwara, S. & Sato, N. Regulatory carbon metabolism underlying seawater-based promotion of triacylglycerol accumulation in *Chlorella kessleri*. *Bioresour. Technol.* **289**, 121686 (2019).

25. Giroud, C., Gerber, A. & Eichenberger, W. Lipids of *Chlamydomonas reinhardtii*. Analysis of molecular species and intracellular site(s) of biosynthesis. *Plant Cell Physiol.* **29**, 587-595 (1988).

552 26. Sato, N., Tsuzuki, M. & Kawaguchi, A. Glycerolipid synthesis in *Chlorella kessleri*
553 11h: I. Existence of a eukaryotic pathway. *Biochim. Biophys. Acta* **1633**, 27–34 (2003).
554 27. Roughan, P.G. & Slack, C.R. Cellular organization of glycerolipid metabolism. *Annu.*
555 *Rev. Plant Physiol.* **33**, 97-132 (1982).
556 28. Roche, S.A. & Leblond, J.D. Betaine lipids in chlorarachniophytes. *Phycol. Res.* **58**,
557 298-305 (2010).
558 29. Riekhof, W.R., Sears, B.B. & Benning, C. Annotations of genes involved in
559 glycerolipid biosynthesis in *Chlamydomonas reinhardtii*: discovery of the betaine
560 lipid synthase $BTA1_{Cr}$. *Eukaryot. Cell* **4**, 242-252 (2005).
561 30. Simocková, M., Holic, R., Tahotná, D., Patton-Vogt, J. & Griac, P. Yeast Pgc1p
562 (YPL206c) controls the amount of phosphatidylglycerol via a phospholipase C-type
563 degradation mechanism. *J. Biol. Chem.* **283**, 17107-15 (2008).
564 31. May, A., Spinka, M. & Köck, M. *Arabidopsis thaliana* PECP1**:** enzymatic
565 characterization and structural organization of the first plant
566 phosphoethanolamine/phosphocholine phosphatase. *Biochim. Biophys. Acta* **1824**,
567 319-325 (2012).

568 32. Hanchi, M. et al. The phosphate fast-responsive genes *PECP1* and *PPsPase1* affect
569 phosphocholine and phosphoethanolamine content. *Plant Physiol.* **176**, 2943-2962
570 (2018).
571 33. Vítová, M., Goecke, F., Sigler, K. & Řezanka, T. Lipidomic analysis of the
572 extremophilic red alga *Galdieria sulphuraria* in response to changes in pH. *Algal Res.*
573 **13**, 218-226 (2016).
574 34. Cañavate, J.P., Armada, I., Ríos, J.L. & Hachero-Cruzado, I. Exploring occurrence
575 and molecular diversity of betaine lipids across taxonomy of marine microalgae.
576 *Phytochem.* **124**, 68-78 (2016).
577 35. López, G. et al. Production of polyunsaturated fatty acids and lipids from autotrophic,
578 mixotrophic and heterotrophic cultivation of *Galdieria* sp. strain USBA-GBX-832. *Sci.*
579 *Rep.* **9**, 10791; 10.1038/s41598-019-46645-3 (2019).
580 36. Sato, N. & Moriyama, N. Genomic and biochemical analysis of lipid biosynthesis in the
581 unicellular rhodophyte *Cyanidioschyzon merolae*: lack of a plastidic desaturation pathway
582 results in the coupled pathway of galactolipid synthesis. *Eukayot. Cell* **6**, 108-111 (2007).
583 37. da Costa, E. et al. High-resolution lipidomics of the early life stages of the red seaweed
584 *Porphyra dioica*. *Molecules* **23**, 187; 10.3390/molecules23010187 (2018).

585 38 Melo, T. et al. Lipidomics as a new approach for the bioprospecting of marine
586 macroalgae – unraveling the polar lipid and fatty acid composition of *Chondrus*
587 *crispus*. *Algal Res.* **8**, 181-191 (2015).
588 39. Riekhof, W.R., Ruckle, M.E., Lydic, T.A., Sears, B.B. & Benning, C. The sulfolipids
589 2'-0-acyl-sulfoquinovosyldiacylglycerol and sulfoquinovosyldiacylglycerol are
590 absent from a *Chlamydomonas reinhardtii* mutant deleted in SQD1. *Plant Physiol.***133**,
591 864-874 (2003).
592 40. Moore, T.S., Du, Z, & Chen, Z. Membrane lipid biosynthesis in *Chlamydomonas*
593 *reinhadrtii*. In vitro biosynthesis of diacylglyceryltrimethylhomoserine. *Plant Physiol.*
594 **125**, 423-429 (2001).
595 41. Härtel, H. & Benning, C. Can digalactosyldiacylglycerol substitute for
596 phosphatidylcholine upon phosphate deprivation in leaves and roots of *Arabidopsis*?
597 *Biochem. Soc. Trans.* **28**, 729-732 (2000).
598 42. Awai, K., Watanabe, H., Benning, C. & Nishida, I. Digalactosyldiacylglycerol is
599 required for better photosynthetic growth of *Synechocystis* sp. PCC6803 under
600 phosphate limitaton. *Plant Cell Physiol.* **48**, 1517-1523 (2007).

601 43. Gaude, N., Nakamura, Y., Scheible, W.R., Ohta, H. & Dörmann, P. Phospholipase
602 C5 (NPC5) is involved in galactolipid accumulation during phosphate limitation in
603 leaves of *Arabidopsis*. *Plant J.* **56**, 28-39 (2008).
604 44. Zavaleta-Pastor, M. et al. *Sinorhizobium meliloti* phospholipase C required for lipid
605 remodeling during phosphorus limitation. *Proc. Natl. Acad. Sci. U.S.A.* **107**, 302-307
606 (2010).
607 45. Verneklaas, E.J. et al. Opportunities for improving phosphorus-use efficiency in crop
608 plants. *New Phytol.* **195**, 306-320 (2012).
609 46. Bariola, P.A., MacIntosh, G.C. & Green, P.J. Regulation of S-like ribonuclease levels
610 in *Arabidopsis*. Antisense inhibition of RNS1 or RNS2 elevates anthocyanin
611 accumulation. *Plant Physiol.* **119**, 331-342 (1999).
612 47. Singh, A., Bhatnagar, N., Pandey, A. & Pandey, G.K. Plant phospholipase C family:
613 Regulation and functional role in lipid signaling. *Cell Calcium* **58**, 139-146 (2015).
614 48. Hiyoshi, T., Oyanagi, K., Niki, T., Fujiwara, S. & Sato, N. Requirement of the
615 exopolyphosphatase gene for cellular acclimation to phosphorus starvation in a
616 cyanobacterium, *Synechocystis* sp. PCC 6803. *Biochem. Biophys. Res. Commun.* **540**,
617 16-21 (2021).

618 49. Shimogawara, K. & Usuda, H. Uptake of inorganic phosphate by suspension-cultured
619 Tobacco cells: kinetics and regulation by Pi starvation. *Plant Cell Physiol.* **36**, 341-
620 351 (1995).
621 50. Sato, N., Kamimura, R., Kaneta, K., Yoshikawa, M. & Tsuzuki, M. Species-specific
622 roles of sulfolipid metabolism in acclimation of photosynthetic microbes to sulfur-
623 starvation stress. *PLoS One* **12**, e0186154; 10.1371/journal.pone.0186154
624 (2017).
625 51. Nguyen, L.T., Schmidt, H.A., von Haeseler, A. & Minh, B.Q. IQ-TREE: a fast and
626 effective stochastic algorithm for estimating maximum-likelihood phylogenies. *Mol.*
627 *Biol. Evol.* **32**, 268-274 (2015).
628 52. Sato, A., Matsumura, R., Hoshino, N., Tsuzuki, M., Sato, N. Responsibility of
629 regulatory gene expression and repressed protein synthesis for triacylglycerol
630 accumulation on sulfur-starvation in *Chlamydomonas reinhardtii*. *Front. Plant Sci.* **5**,
631 444; 10.3389/fpls.2014.00444 (2014).
632
633
634 **Acknowledgements**

635 The authors are deeply grateful to Prof. Eiji Suzuki (Akita Prefectural University) for
636 his kind providing of information on the *Chlorella kessleri* genomic DNA sequences. N.S.
637 was financially supported by SEI Group CSR Foundation and Grant-in-Aid for Scientific
638 Research (C) from Japan Society for the Promotion of Science (19K12384).
639
640
641 **Author contributions**
642
643 Y.O., R.O., Y.I., E.K., M.A. and N.S. performed research; Y.O., R.O., Y.I., E.K., M.A.,
644 M.T., S.F. and N.S. analyzed data; N.S. provided supervision, and drafted the manuscript,
645 and all authors read and approved the final version..
646
647
648 **Additional information**
649
650 Supplementary information accompanies this paper.
651
652 Competing interests: The authors declare no competing interests.

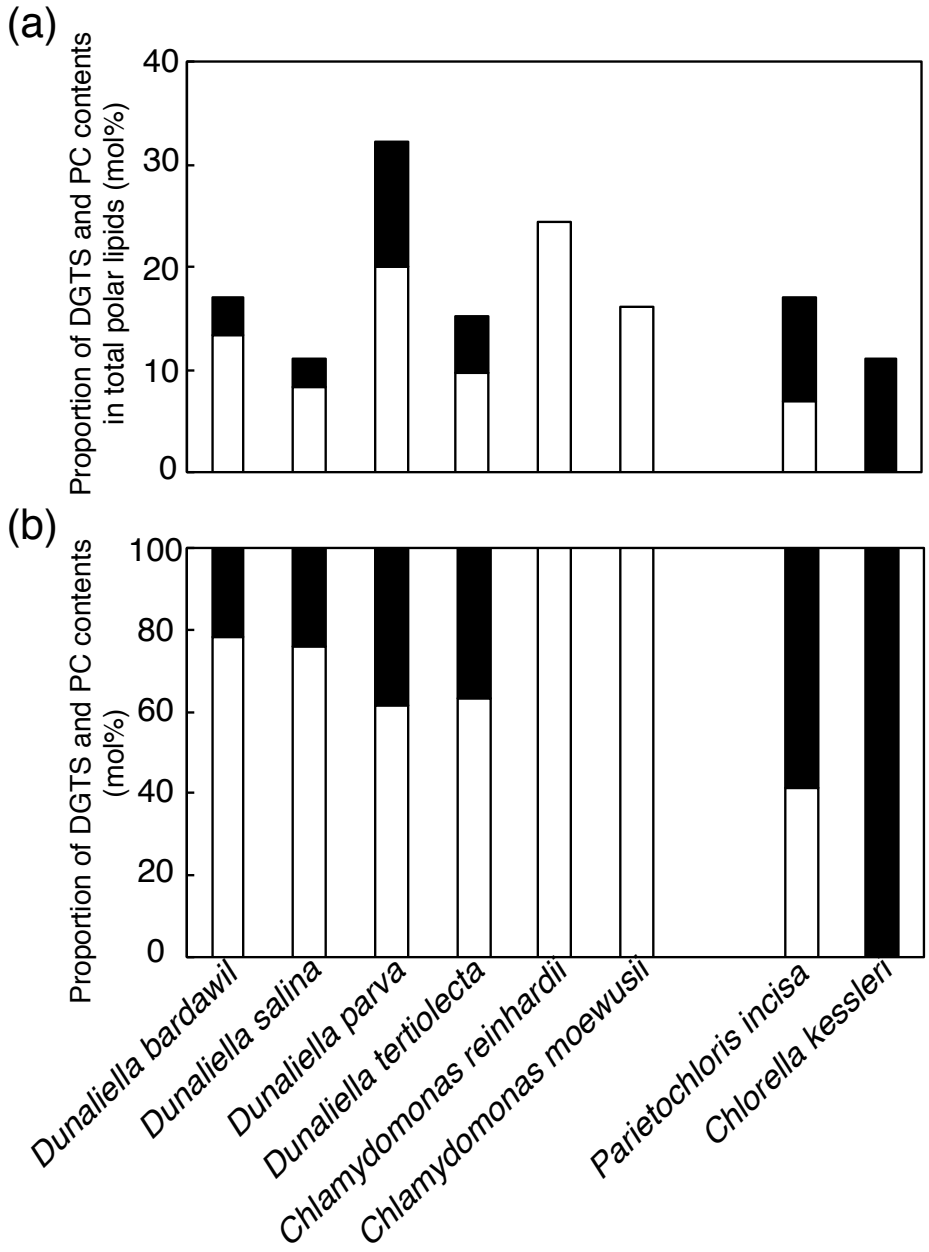

653

654

655 Fig. 1 DGTS and PC contents in green algae grown under +P conditions. (a) Respective
656 contents of DGTS and PC relative to that of total polar lipids. (b) The proportion of DGTS
657 and PC contents. White and black bars indicate the contents of DGTS and PC,
658 respectively. The values were obtained from previous reports (10-15,17).

659

660

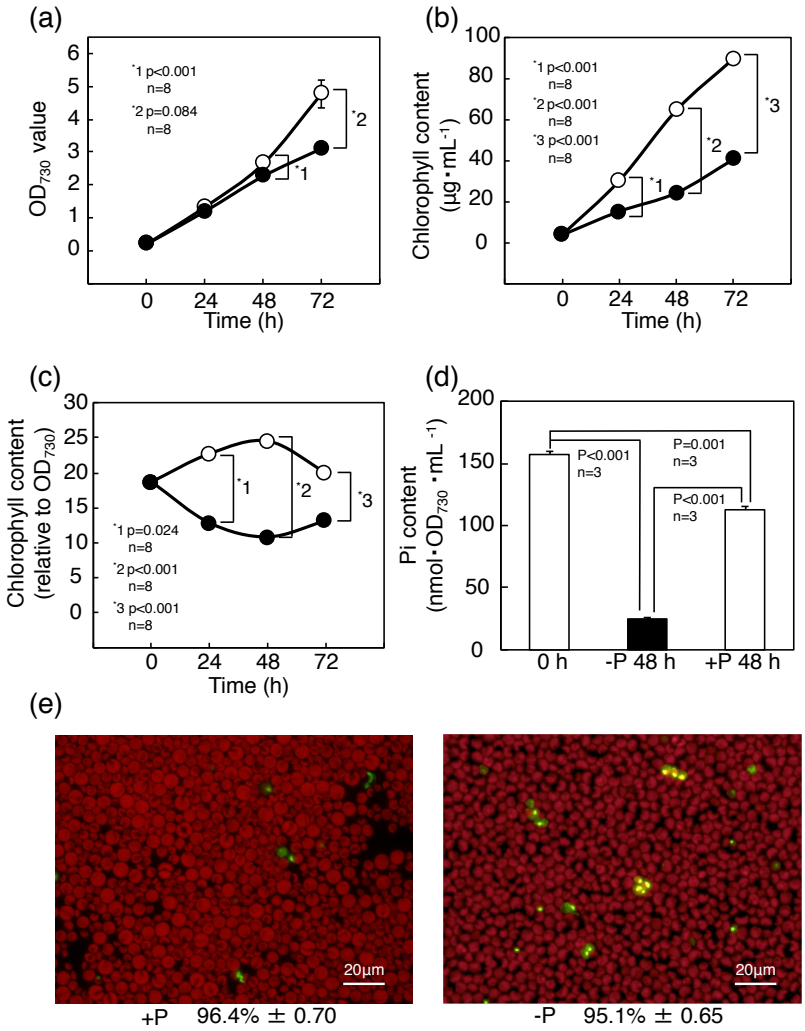

Fig. 2 Effects of -P stress on physiological behavior in *C. kessleri* cells. (a) Cell growth on the basis of the OD_{730} value of the culture. (b) Chl content in the culture. (c) The cellular Chl content obtained through estimation of the relative ratios of the values in (b) to those in (a). White and black circles indicate cells grown under +P and -P conditions, respectively. (d) Pi contents measured in cells grown under +P conditions (0 h), and in ones grown further for 48 h under + P and -P conditions. (e) Images of the cells emitting red auto-fluorescence of Chl and/or the green fluorescence of SYTOX bound to chromosomal DNA. The survival ratio of the cells was determined through estimation of the proportion of the number of viable cells emitting only red fluorescence, relative to that of total cells, including non-viable cells with emission of green fluorescence only and with that of both red and green fluorescence. The values shown are averages ± SEM for two technical replicates for each of four biological replicates (a-c), and those for three biological replicates (d, e). Data were analyzed by one-tailed Student's *t*-test.

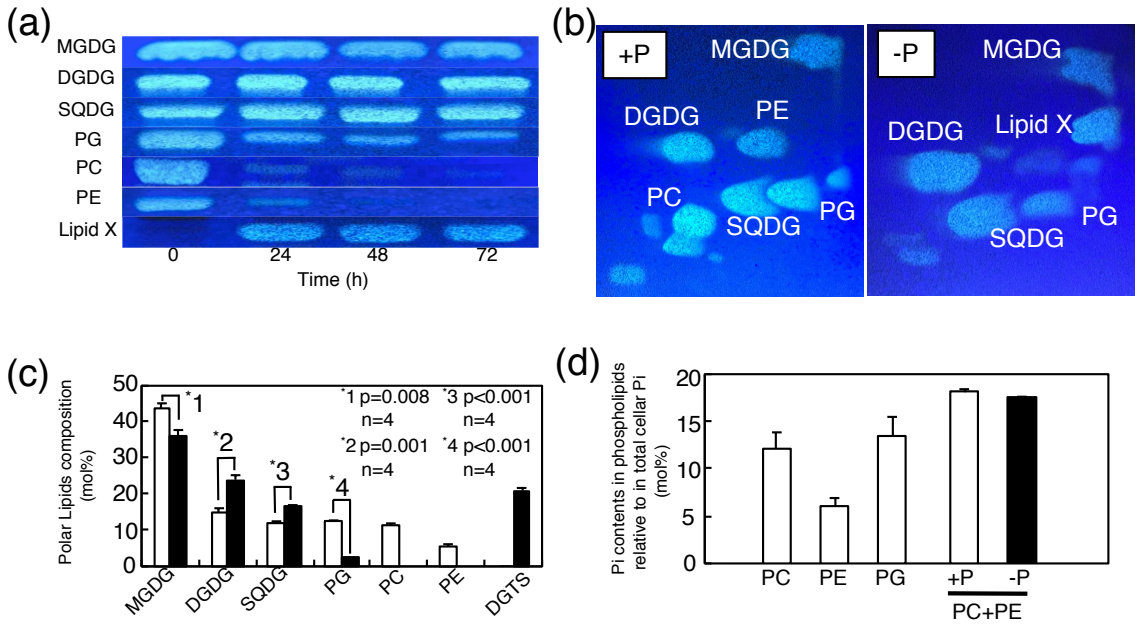

Fig. 3 Lipid remodeling in *C. kessleri* cells in response to -P stress. (a) Qualitative TLC analysis of individual polar lipids prepared from cells grown under +P conditions (0 h), and from ones shifted to -P conditions for further growth for 24, 48, and 72 h. (b) Two-dimensional TLC profile of polar lipids in the cells grown for 48 h under +P or -P conditions. (c) Polar lipid composition in the cells grown for 48 h under +P (white bars) or -P conditions (black bars). (d) The contents of Pi included in individual phospholipids, relative to that in total cellular fraction. The values shown are averages ± SEM for two technical replicates for each of two biological replicates (c), and those estimated on the basis of the data in Fig. 2d and Fig. 3c (d). Data were analyzed by one-tailed Student's *t*-test.

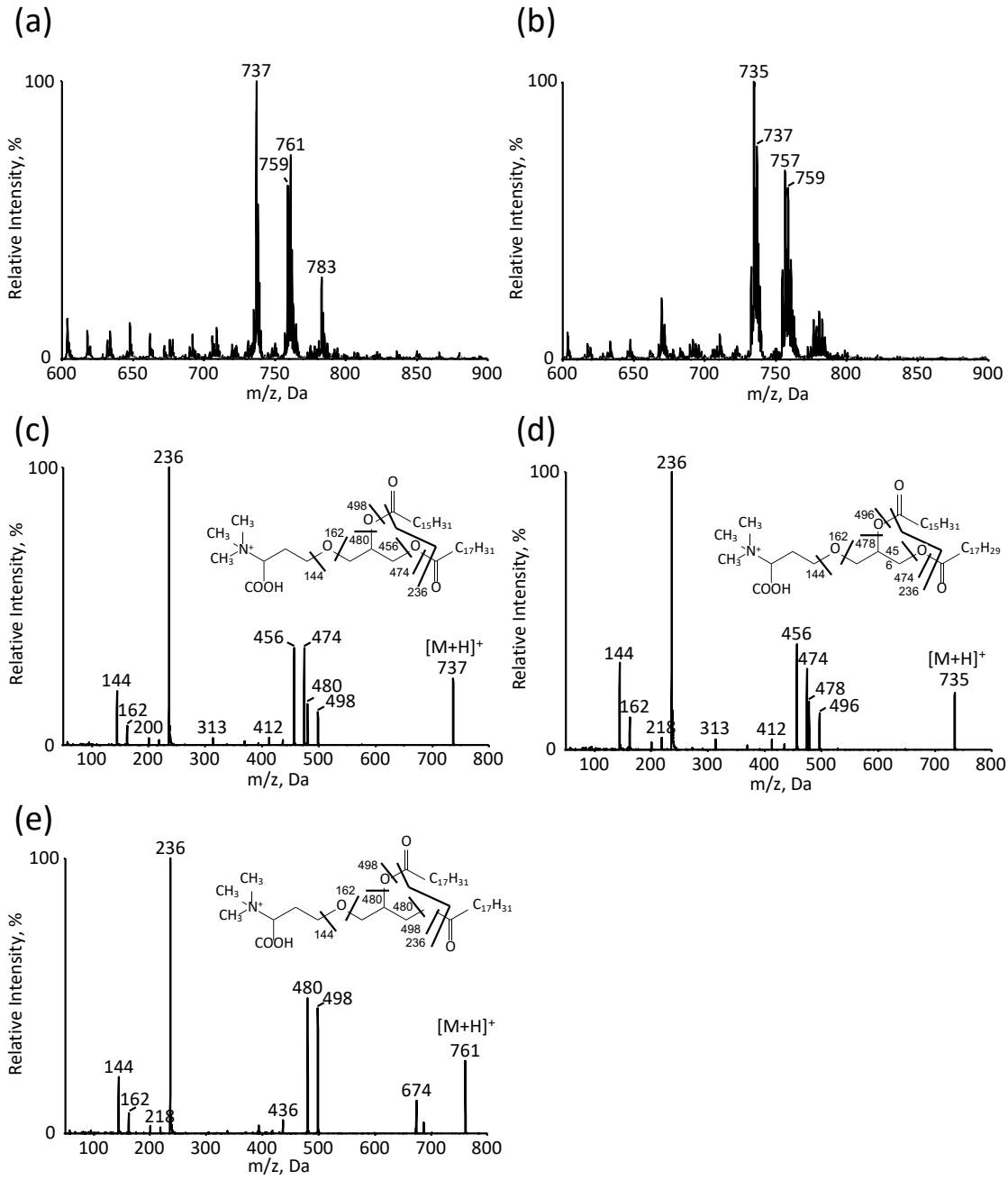

Fig. 4 Identification of a -P-induced novel lipid as DGTS through LC/MS^2 analysis. ESI mass spectra as to a novel lipid of *C. kessleri* (a) and DGTS of *C. reinharditii* (b). Product ion spectra (c), (d), and (e), as to m/z 737 in (a), m/z 735 in (b), and m/z 761 in (a), respectively.

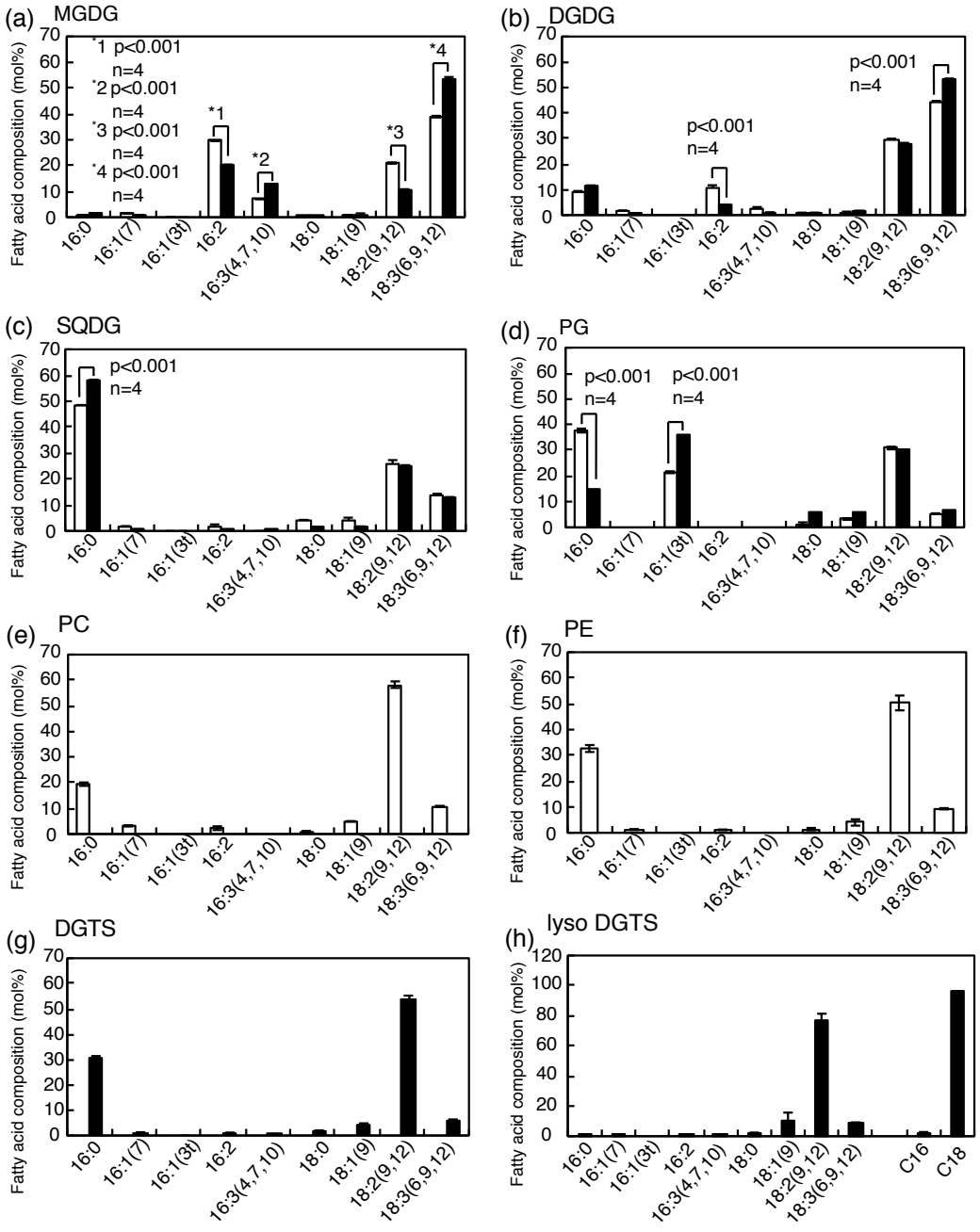

Fig. 5 Fatty acid composition of individual polar lipids. The fatty acid compositions of MGDG (a), DGDG (b), SQDG (c), and PG (d) are shown for 48-h grown +P (black bars) and -P cells (white bars), whereas those of PC (e) and PE (f), and DGTS (g) are for +P and -P cells, respectively. The fatty acid composition of *sn*-2 monoacyl lysoDGTS is shown in (h). The values shown are averages ± SEM for two technical replicates for each of two biological replicates. Data were analyzed by one-tailed Student's *t*-test.

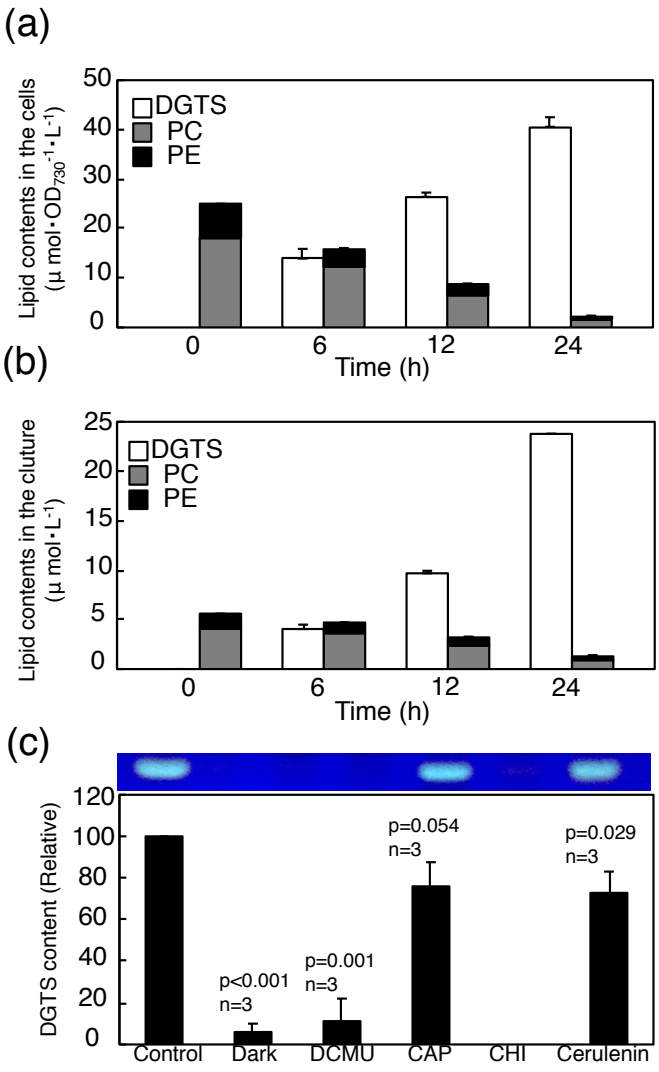

705

706

707 Fig. 6 Metabolic mechanism of DGTS accumulation under -P conditions. Changes in
708 the contents of DGTS (white), PC (grey), and PE (black) in cells grown for 12 h after a
709 shift from +P to -P conditions, which were estimated in cells on an OD_{730} ml culture basis
710 (a), and in the culture (b). (c) Effects of metabolic inhibitors or light conditions on the
711 accumulation of DGTS in the cells shifted to -P conditions. The values were estimated as
712 the proportion of the DGTS content in the cells with application of chloramphenicol
713 (CAP), cycloheximide (CHI), cerulenin, and DCMU, and in those shifted to the dark
714 conditions, relative to that in non-treated control cells. The values shown are
715 averages ± SEM for three biological replicates. Data were analyzed by one-tailed
716 Student's *t*-test.

717

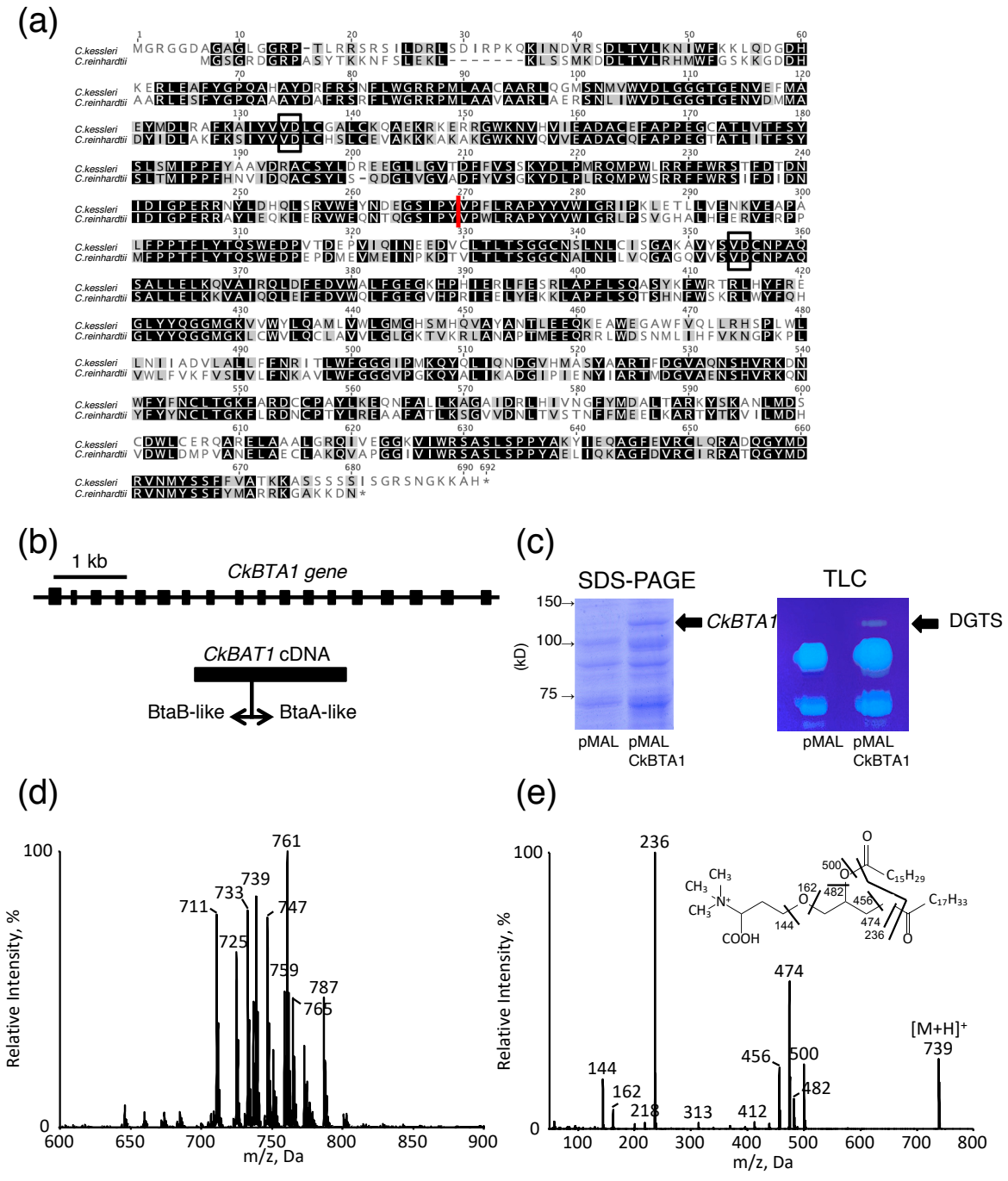

Fig. 7 Structural and functional identification of a BTA1 homolog in *C. kessleri*. (a) Alignment of the postulated amino acid sequence of a BTA1 homolog with that of CrBTA1. Identical and similar amino acid residues are shadowed in black and grey. The vertical red line indicates the boundary of the N-terminal BtaB- and C-terminal BtaA-like domains, whereas two black boxes shows the conserved dipeptide VD for the binding of SAM, the substrate in the respective catalytic actions of BtaA and BtaB. (b) The structure of the of the *BTA1* homolog of *C. kessleri*. The *BTA1* homolog is composed of 18 exons

on the nuclear genome. (c) Expression of cDNA of the *BTA1* homolog in *E. coli.* SDS-PAGE of total cellular proteins shows induction of the expression of the homolog protein in pMAL-*CkBTA1* introduced *E. coli* cells, but not in empty-vector introduced ones. TLC of total cellular lipids shows the appearance of a novel lipid specifically in pMAL-*CkBTA1* introduced *E. coli* cells. (d) The ESI mass spectrum of the novel lipid in the transformant of *E. coli*. (e) The product ion spectrum of m/z 739 in (d). Note that the product ion spectrum exhibited three signals (m/z 144, 162 and 236) for identification of the novel lipid as DGTS.

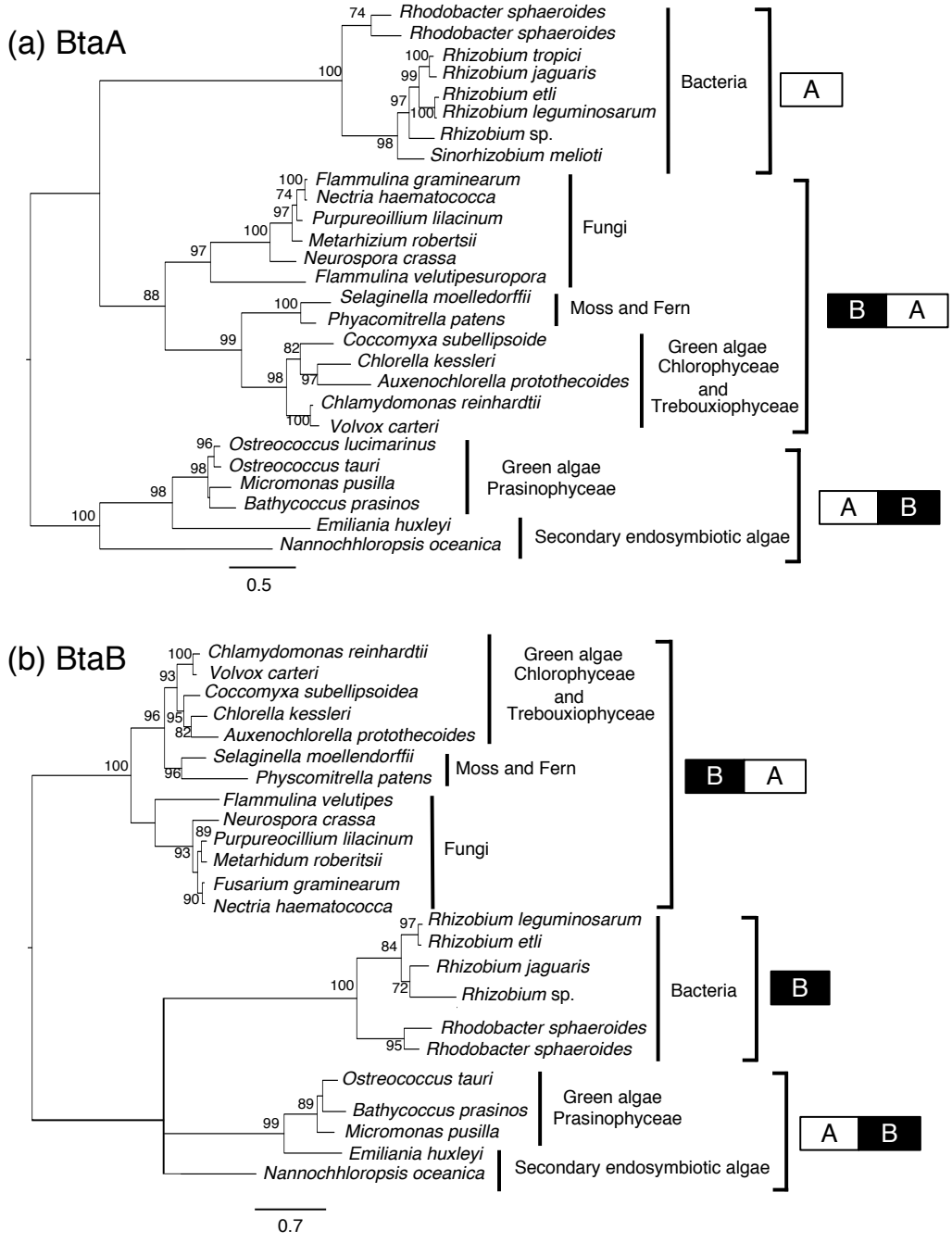

734

735 Fig. 8 Phylogenetic trees of the BtaA and BtaB domains in BTA1 proteins. (a) Bacterial
736 BtaA and eukaryotic BtaA-domains. (b) Bacterial BtaB and eukaryotic BtaB-domains.
737 Two linked boxes, AB and BA, indicate eukaryotic A and B type BTA1 proteins,
738 respectively, whereas single boxes, A and B, demonstrate bacterial BtaA and BtaB
739 proteins, respectively.

740

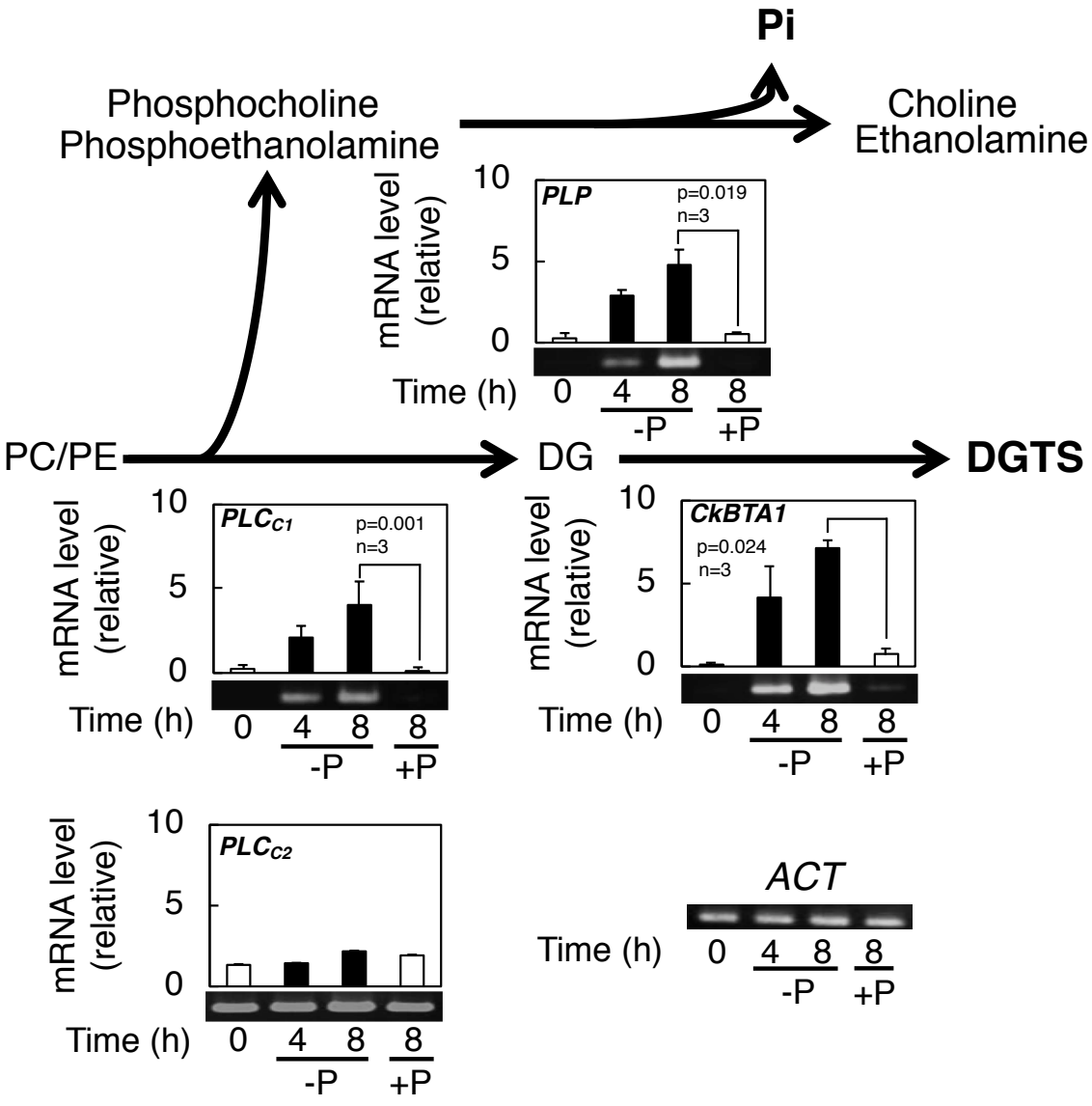

741

742

743 Fig. 9 Regulatory expression of the genes for -P induced lipid remodeling in *C. kessleri*.
744 The expression levels of the *BTA1*, PLC_{C1}, PLC_{C2}, and *PLP* genes were investigated
745 through semi-quantitative RT-PCR analysis in *C. kessleri* cells before and after a shift to
746 -P conditions. The intensities of the DNA bands that correspond to mRNAs of the
747 individual genes were used for determination of the values, relative to that of *ACT*. The
748 values shown are averages ± SEM for three biological replicates. Data were analyzed by
749 one-tailed Student's *t*-test.

750

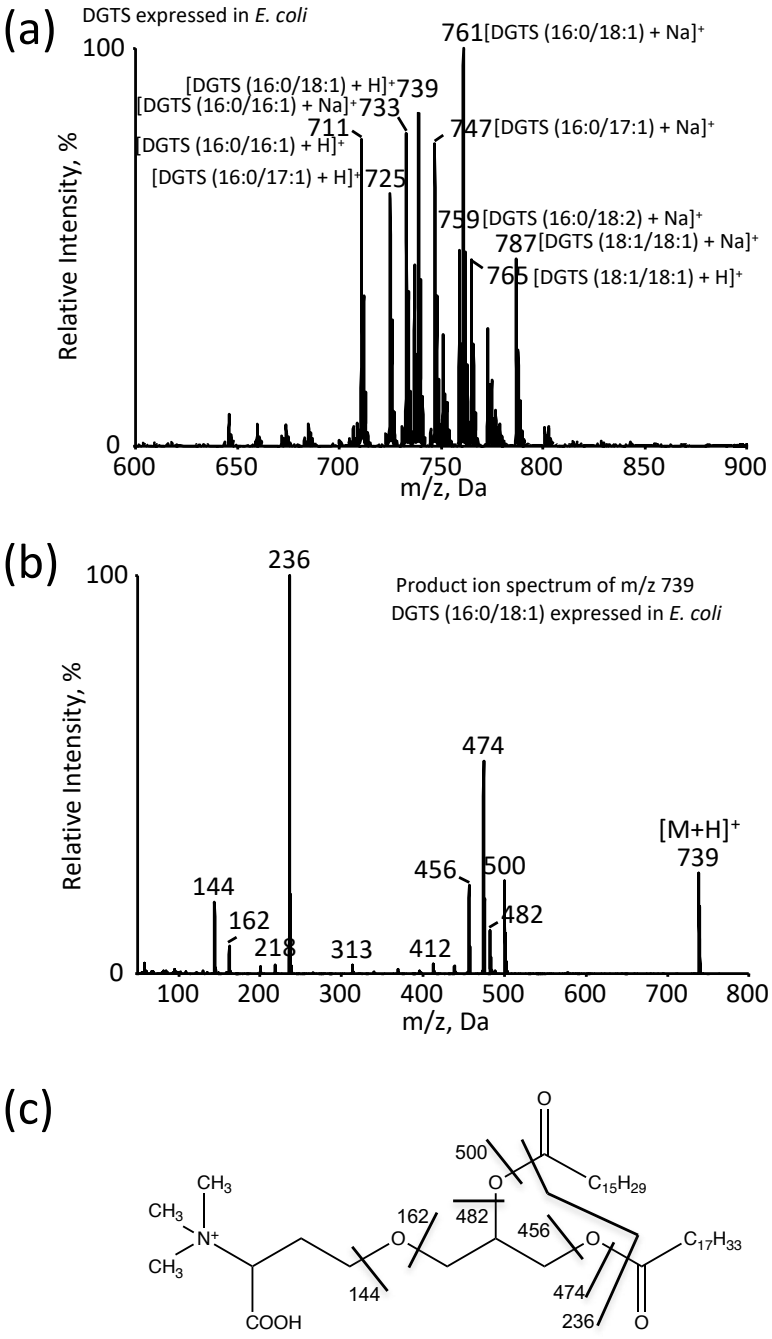

Supplementary Fig. 1 Mass spectrometric identification of DGTS. (a) ESI mass spectra of DGTS expressed in *E. coli*. (b) Product ion spectrum of m/z 739 at (a). (c) Estimated fragmentation pattern for DGTS (16:0/18:1) from the product ion spectrum, in which the *sn* position of fatty acids is provisional.

751

752

Supplementary Table 1 Primer set

set	gene	Forward	Reverse	Query
1	*5′ race cDNA*	ctaatacgactcactatagggcaagcagtggtatcaacgcagag	gattacgccaagcttcagtcactgggtcctcccacgact	
2	*3′ race cDNA*	gattacgccaagctttcttcccgcccaccttcctgtac	ctaatacgactcactatagggcaagcagtggtatcaacgcagag	
3	*CkBTA1*	gcgcagactaattcgatgggacgcggtggagat	tgttgttgttgttcgtcagtgggccttcttgcc	
4	*BTA1*	tcctctaagtacgacctccc	tccagaacttgtaggacgcc	Cre.07.g324200.t1.2
5	*PLCC1*	gctctcatggtagccgactc	tttagctccttcgaccctga	Cre03.g203600.t1.2
6	*PLCC2*	catcttccctgaccacac	ccgttgaatgcctggttg	Cre16.g683850.t1.3
7	*PLP*	caccctaccatgagtgcag	gccagcacaacgtcttgc	AT1G17710
8	*ACT*	agaaggacacttacattggc	cagagtcaagcacaataccg	AB046457.1

753

754

Supplementary Table 2 BtaA, BtaB, and BTA1 homologs

	Organisms	gene ID
BtaA	**Bacteria**	
	Rhodobacter sphaeroides	ATCC 17025 (Rsph17025_3617)
	Rhizobium sp S41	BA939_05055
	Rhizobium leguminosarum bv. trifolii WSM2304	Rleg2_2613
	Rhizobium jaguaris	CCGE525_12990
	Rhizobium tropici	RTCIAT899_CH11455
	Rhizobium etli bv. mimosae Mim1	REMIM1_CH02915
	Sinorhizobium meliloti	NP_386300
BtaB	**Bacteria**	
	Rhodobacter sphaeroides ATCC	Rsph17025_3616
	Rhizobium-sp NT-26	NT26_2169
	Rhizobium leguminosarum bv. trifolii WSM2304	*Rleg2_2614*
	Rhizobium jaguaris	CCGE525_12995
	Rhizobium etli by phaseoli	IE4803_CH03093
BTA1	**Green algae**	
	Chlamydomonas reinhardtii	CHLREDRAFT_77062
	Coccomyxa subellipsoidea	COCSUDRAFT_28345
	Auxenochlorella protothecoides	F751_5248
	Volvox carteri f. nagariensis	VOLCADRAFT_83033
	Ostreococcus lucimarinus	OSTLU_27669
	Ostreococcus tauri	OT_ostta15g02860
	Micromonas pusilla	MICPUCDRAFT_48920
	Bathycoccus prasinos	Bathy08g00260
	Monoraphidium neglectum	MNEG_12083
	Fern	
	Selaginella moellendorffii	SELMODRAFT_429378
	Moss	
	Physcomitrella patens subsp. Patens	112274025
	Secondary endosymbiotic algae	
	Emiliania huxleyi	CCMP1516
	Nannochloropsis oceanica	LC375792
	Fungi	
	Metarhizium robertsii	MAA_07461
	Purpureocillium lilacinum	VFPFJ_09846
	Colletotrichum fioriniae	CFIO01_08357
	Nectria haematococc a	NECHADRAFT_31251
	Fusarium graminearum	FGSG_00742
	Flammulina velutipes	KM668875
	Neurospora crassa	NCU03032

Figures

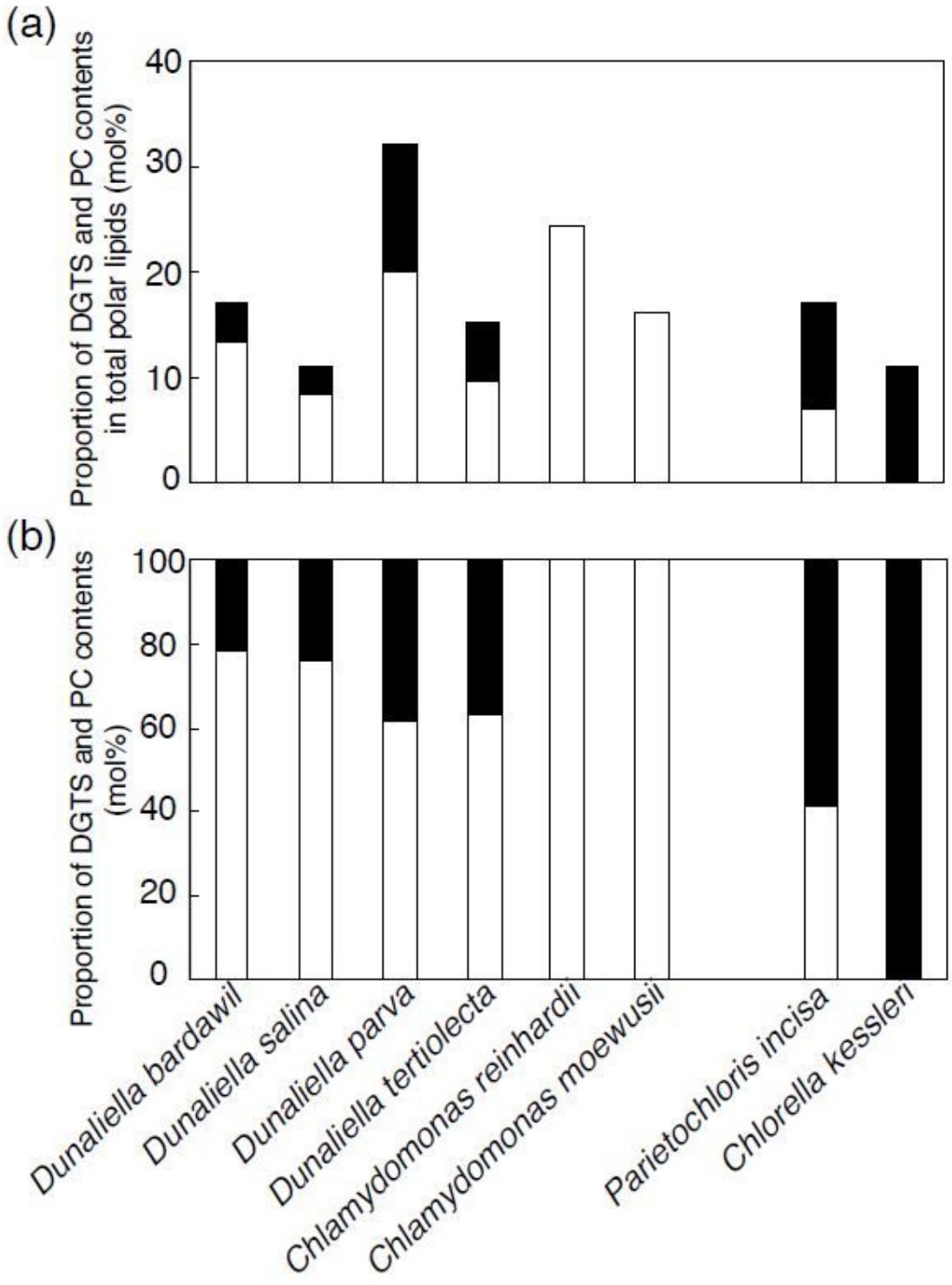

Figure 1

DGTS and PC contents in green algae grown under +P conditions. (a) Respective contents of DGTS and PC relative to that of total polar lipids. (b) The proportion of DGTS and PC contents. White and black bars

indicate the contents of DGTS and PC, respectively. The values were obtained from previous reports (10-15,17).

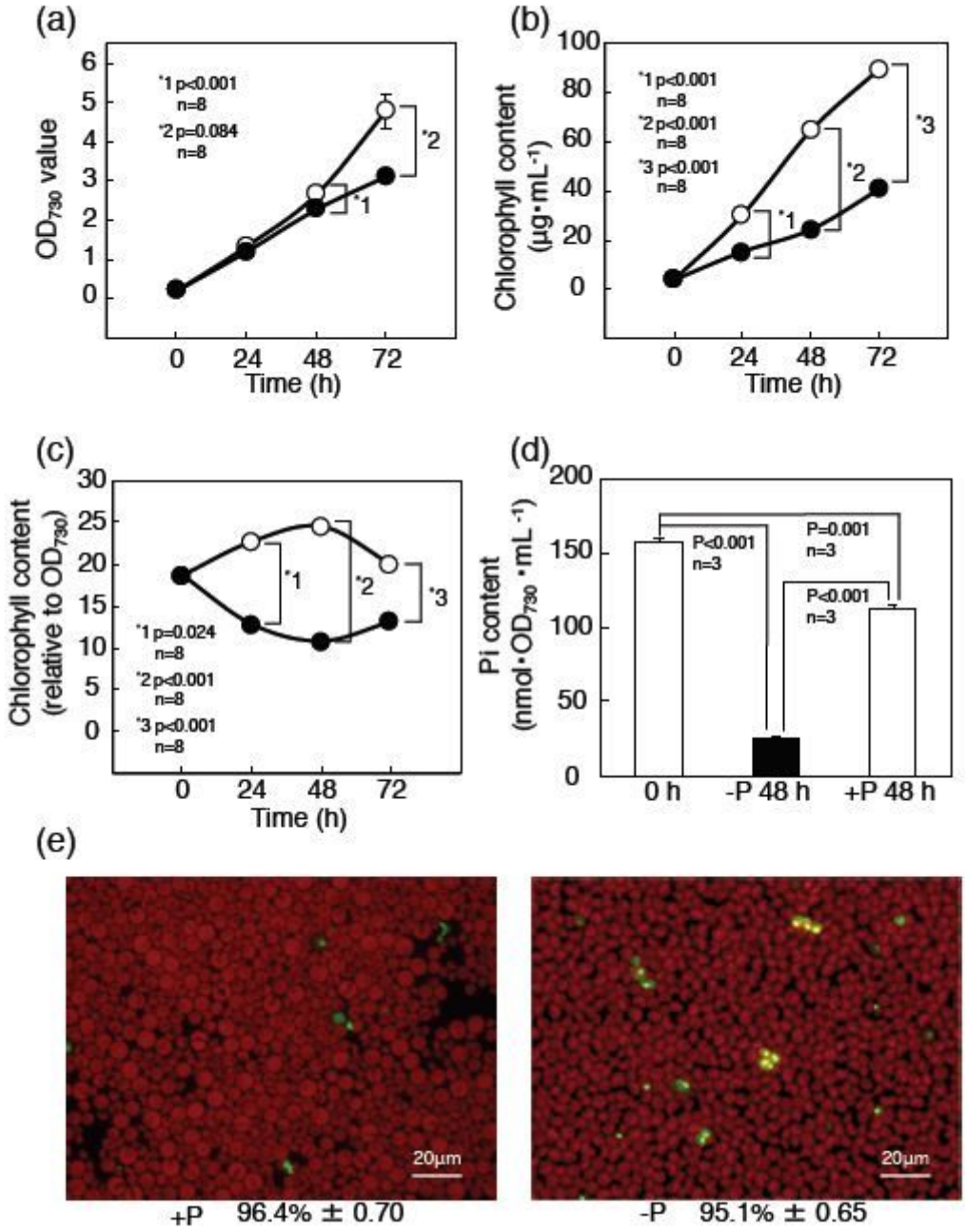

Figure 2

Effects of -P stress on physiological behavior in C. kessleri cells. (a) Cell growth on the basis of the OD730 value of the culture. (b) Chl content in the culture. (c) The cellular Chl content obtained through estimation of the relative ratios of the values in (b) to those in (a). White and black circles indicate cells grown under +P and -P conditions, respectively. (d) Pi contents measured in cells grown under +P conditions (0 h), and in ones grown further for 48 h under + P and -P conditions. (e) Images of the cells emitting red auto-fluorescence of Chl and/or the green fluorescence of SYTOX bound to chromosomal

DNA. The survival ratio of the cells was determined through estimation of the proportion of the number of viable cells emitting only red fluorescence, relative to that of total cells, including non-viable cells with emission of green fluorescence only and with that of both red and green fluorescence. The values shown are averages ± SEM for two technical replicates for each of four biological replicates (a-c), and those for three biological replicates (d, e). Data were analyzed by one-tailed Student's t-test.

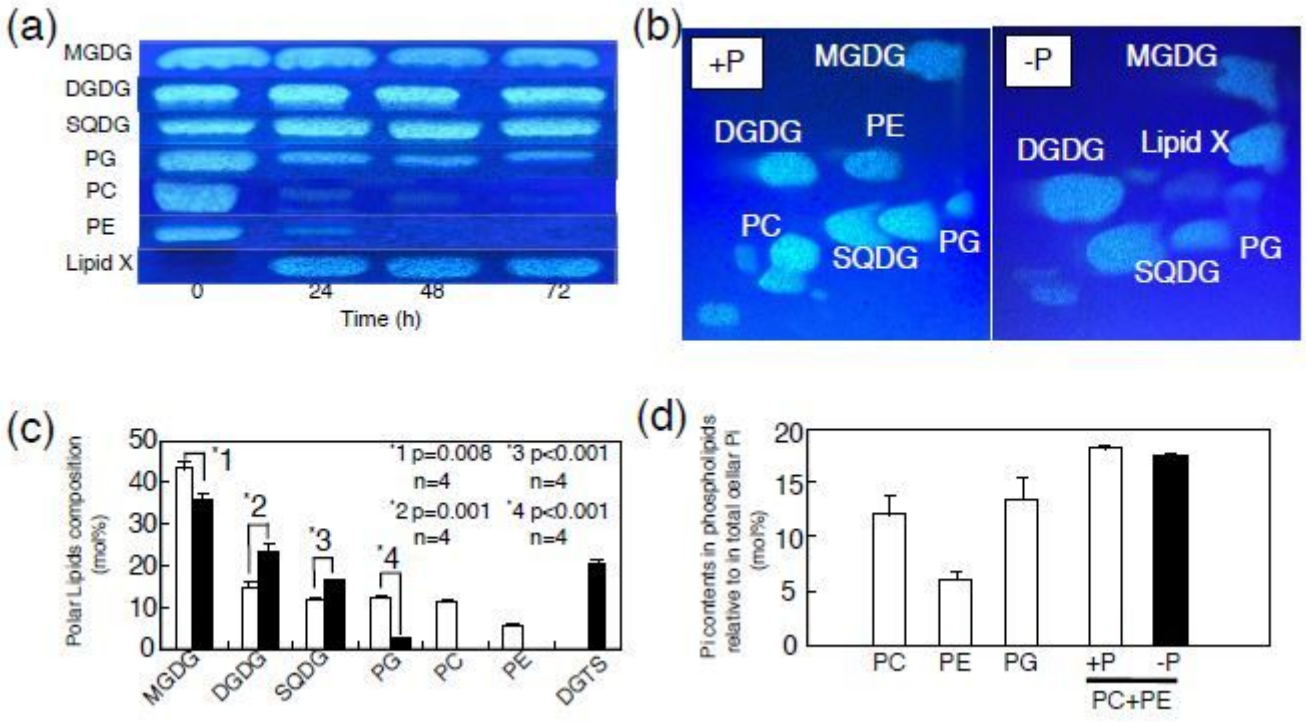

Figure 3

Lipid remodeling in C. kessleri cells in response to -P stress. (a) Qualitative TLC analysis of individual polar lipids prepared from cells grown under +P conditions (0 h), and from ones shifted to -P conditions for further growth for 24, 48, and 72 h. (b) Two-dimensional TLC profile of polar lipids in the cells grown for 48 h under +P or -P conditions. (c) Polar lipid composition in the cells grown for 48 h under +P (white bars) or -P conditions (black bars). (d) The contents of Pi included in individual phospholipids, relative to that in total cellular fraction. The values shown are averages ± SEM for two technical replicates for each of two biological replicates (c), and those estimated on the basis of the data in Fig. 2d and Fig. 3c (d). Data were analyzed by one-tailed Student's t-test.

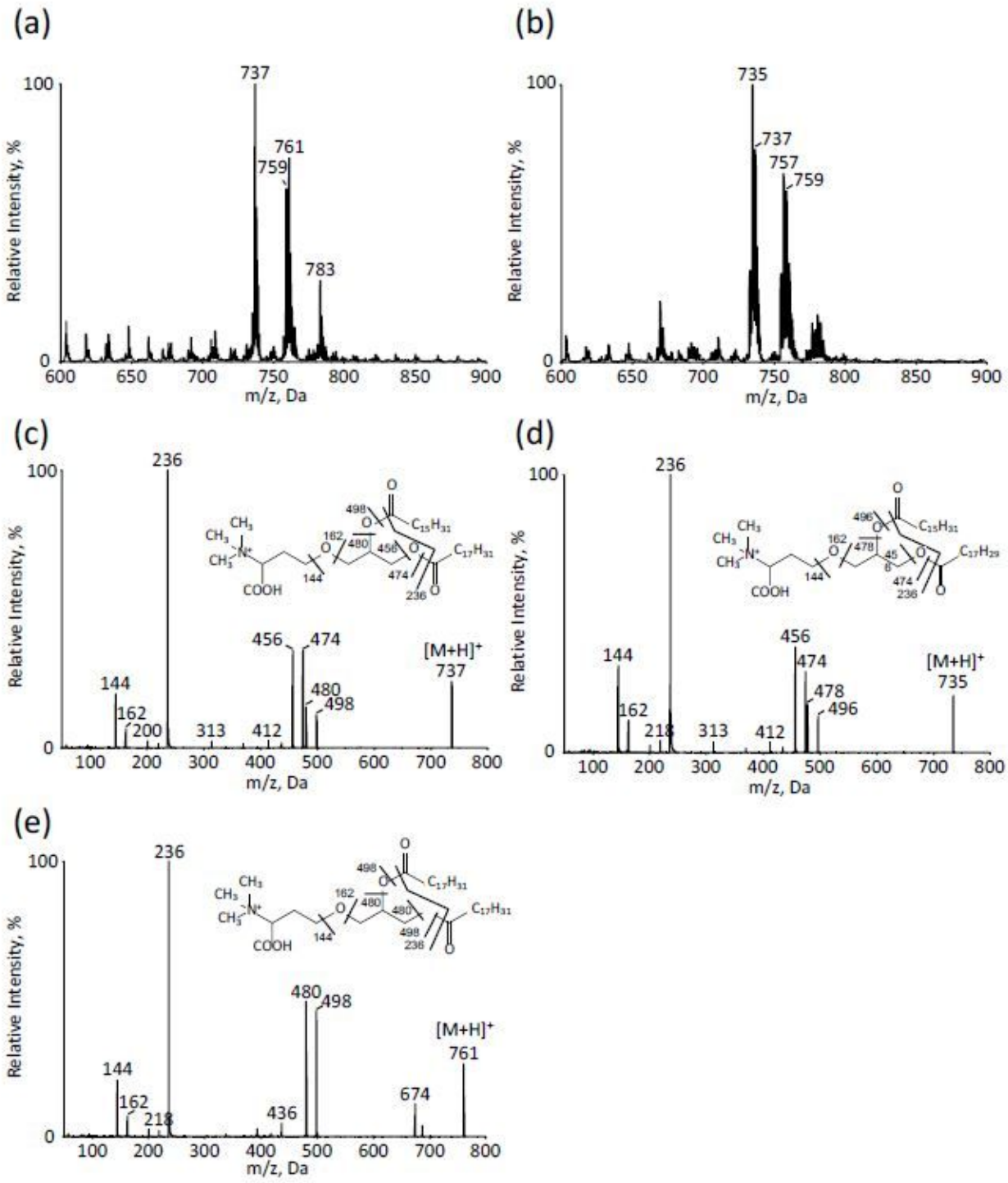

Figure 4

Identification of a -P-induced novel lipid as DGTS through LC/MS2 analysis. ESI mass spectra as to a novel lipid of C. kessleri (a) and DGTS of C. reinharditii (b). Product ion spectra (c), (d), and (e), as to m/z 737 in (a), m/z 735 in (b), and m/z 761 in (a), respectively.

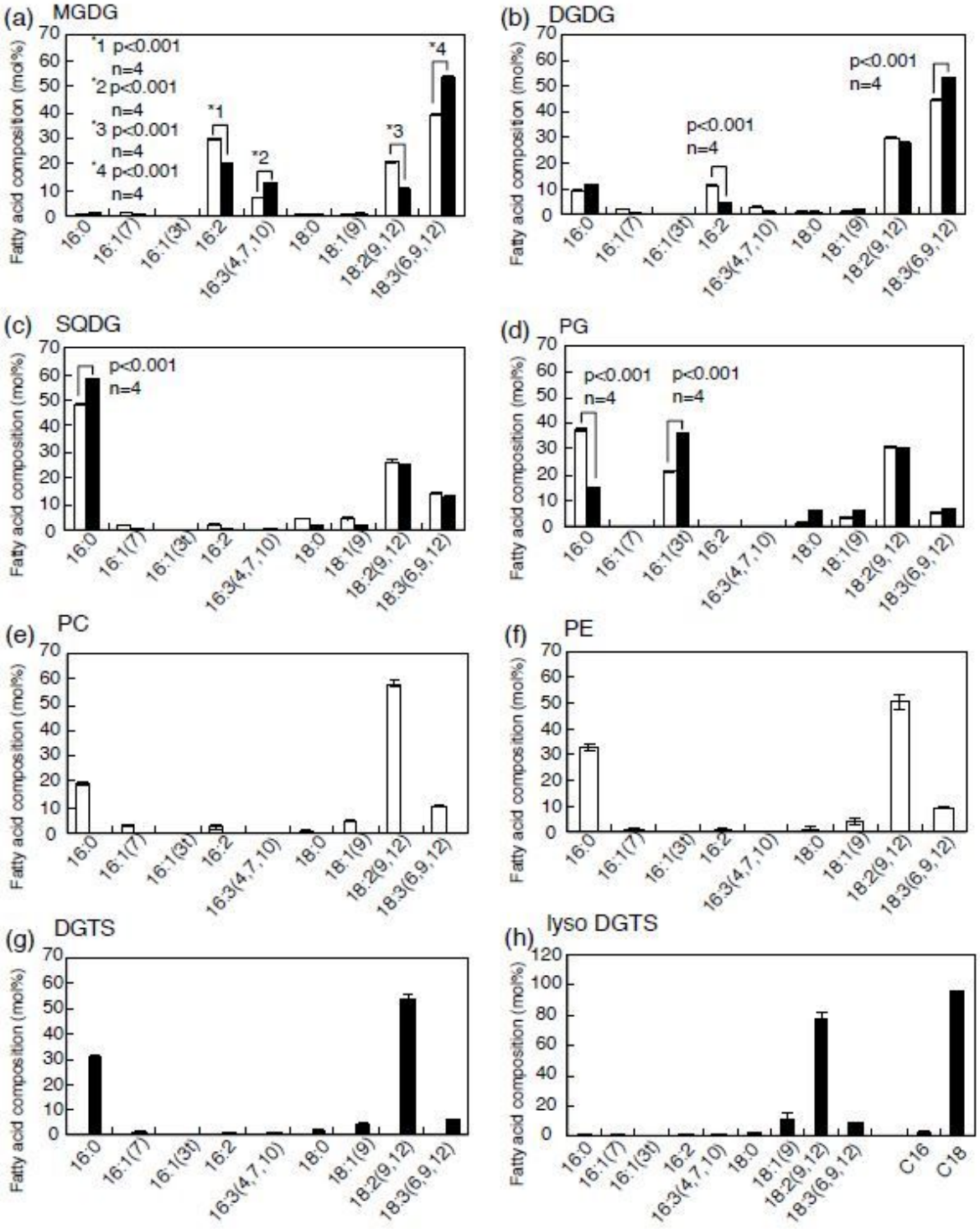

Figure 5

Fatty acid composition of individual polar lipids. The fatty acid compositions of MGDG (a), DGDG (b), SQDG (c), and PG (d) are shown for 48-h grown +P (black bars) and -P cells (white bars), whereas those of PC (e) and PE (f), and DGTS (g) are for +P and -P cells, respectively. The fatty acid composition of sn-2 monoacyl lysoDGTS is shown in (h). The values shown are averages ± SEM for two technical replicates for each of two biological replicates. Data were analyzed by one-tailed Student's t-test.

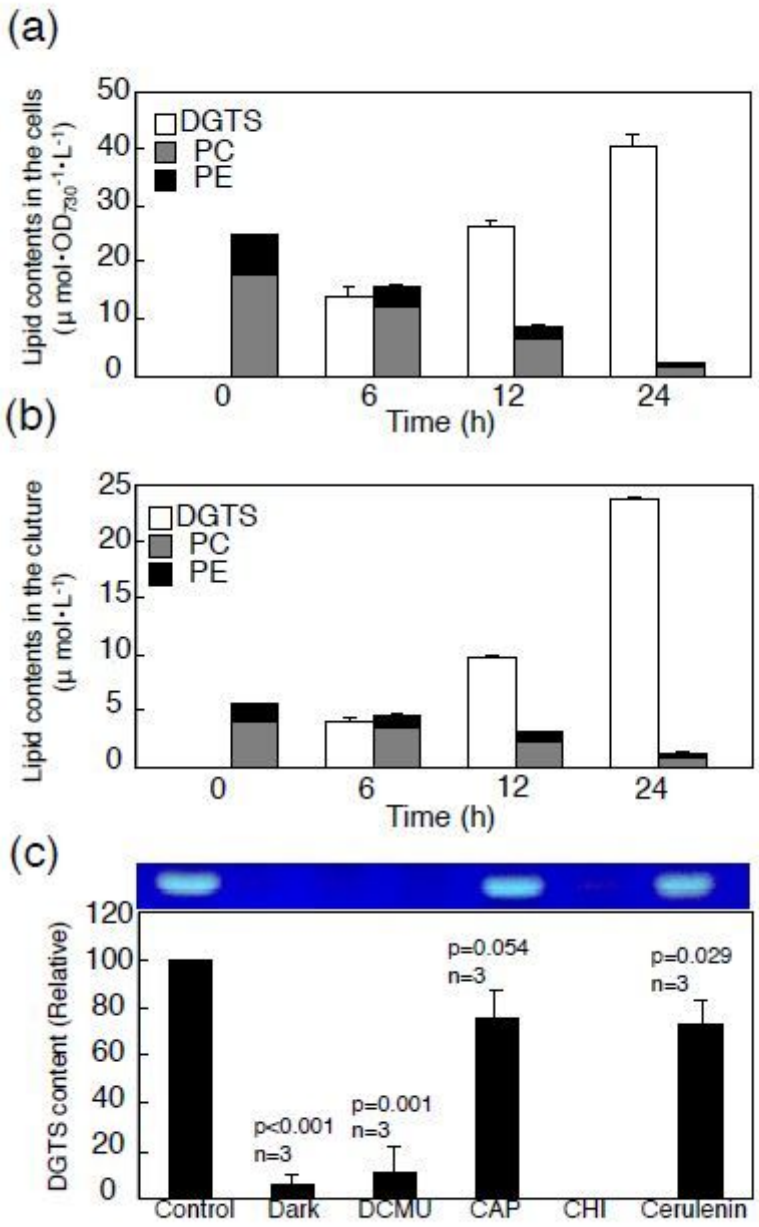

Figure 6

Metabolic mechanism of DGTS accumulation under -P conditions. Changes in the contents of DGTS (white), PC (grey), and PE (black) in cells grown for 12 h after a shift from +P to -P conditions, which were estimated in cells on an OD730 ml culture basis (a), and in the culture (b). (c) Effects of metabolic inhibitors or light conditions on the accumulation of DGTS in the cells shifted to -P conditions. The values were estimated as the proportion of the DGTS content in the cells with application of chloramphenicol (CAP), cycloheximide (CHI), cerulenin, and DCMU, and in those shifted to the dark conditions, relative to that in non-treated control cells. The values shown are averages ± SEM for three biological replicates. Data were analyzed by one-tailed Student's t-test.

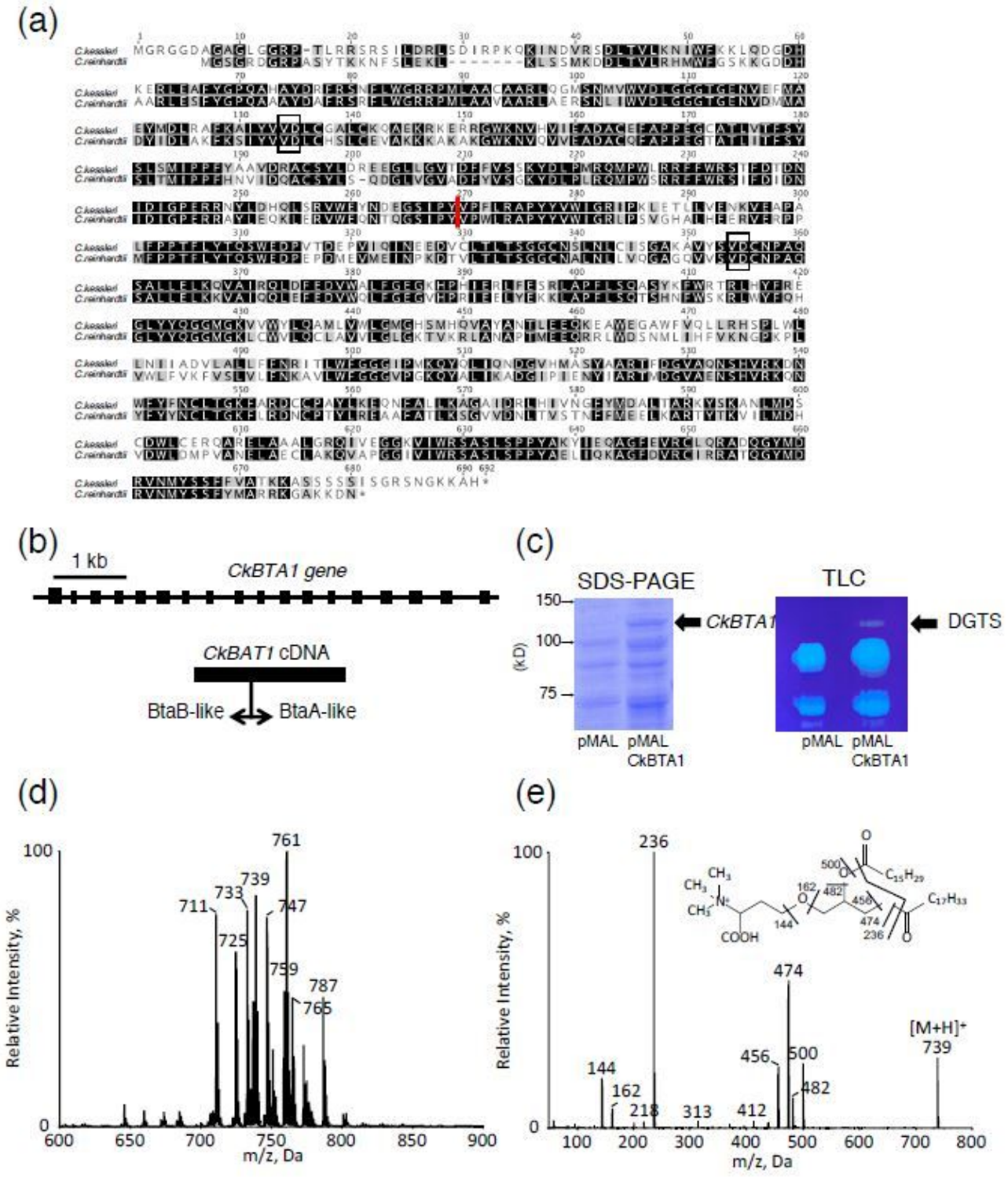

Figure 7

Structural and functional identification of a BTA1 homolog in C. kessleri. (a) Alignment of the postulated amino acid sequence of a BTA1 homolog with that of CrBTA1. Identical and similar amino acid residues are shadowed in black and grey. The vertical red line indicates the boundary of the N-terminal BtaB- and C-terminal BtaA-like domains, whereas two black boxes shows the conserved dipeptide VD for the binding of SAM, the substrate in the respective catalytic actions of BtaA and BtaB. (b) The structure of the of the

BTA1 homolog of C. kessleri. The BTA1 homolog is composed of 18 exons on the nuclear genome. (c) Expression of cDNA of the BTA1 726 homolog in E. coli. SDS PAGE of total cellular proteins shows induction of the expression of the homolog protein in pMAL-CkBTA1 introduced E. coli cells, but not in empty-vector introduced ones. TLC of total cellular lipids shows the appearance of a novel lipid specifically in pMAL CkBTA1 introduced E. coli cells. (d) The ESI mass spectrum of the novel lipid in the transformant of E. coli. (e) The product ion spectrum of m/z 739 in (d). Note that the product ion spectrum exhibited three signals (m/z 144, 162 and 236) for identification of the novel lipid as DGTS.

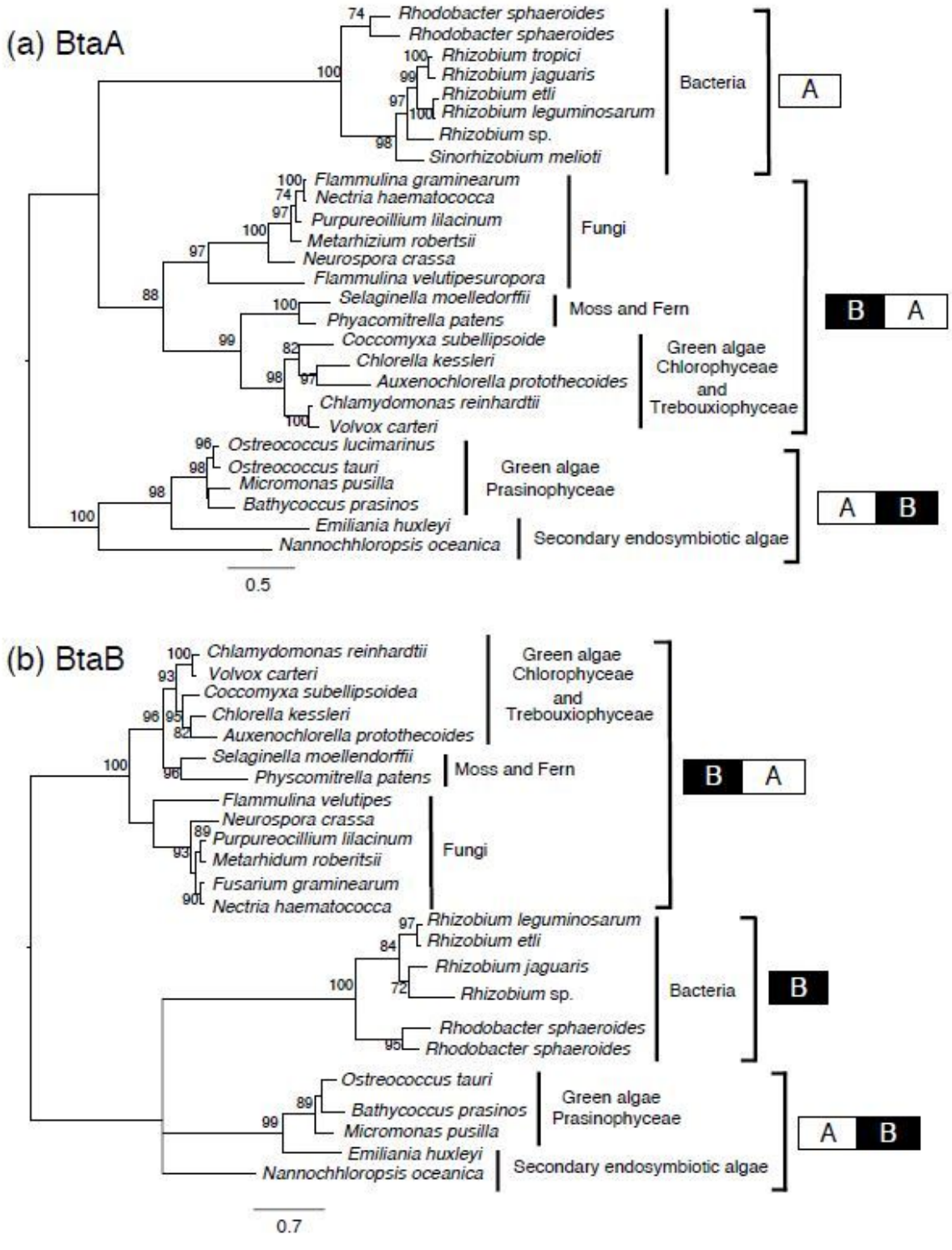

Figure 8

Phylogenetic trees of the BtaA and BtaB domains in BTA1 proteins. (a) Bacterial BtaA and eukaryotic BtaA-domains. (b) Bacterial BtaB and eukaryotic BtaB-domains. Two linked boxes, AB and BA, indicate eukaryotic A and B type BTA1 proteins, respectively, whereas single boxes, A and B, demonstrate bacterial BtaA and BtaB proteins, respectively.

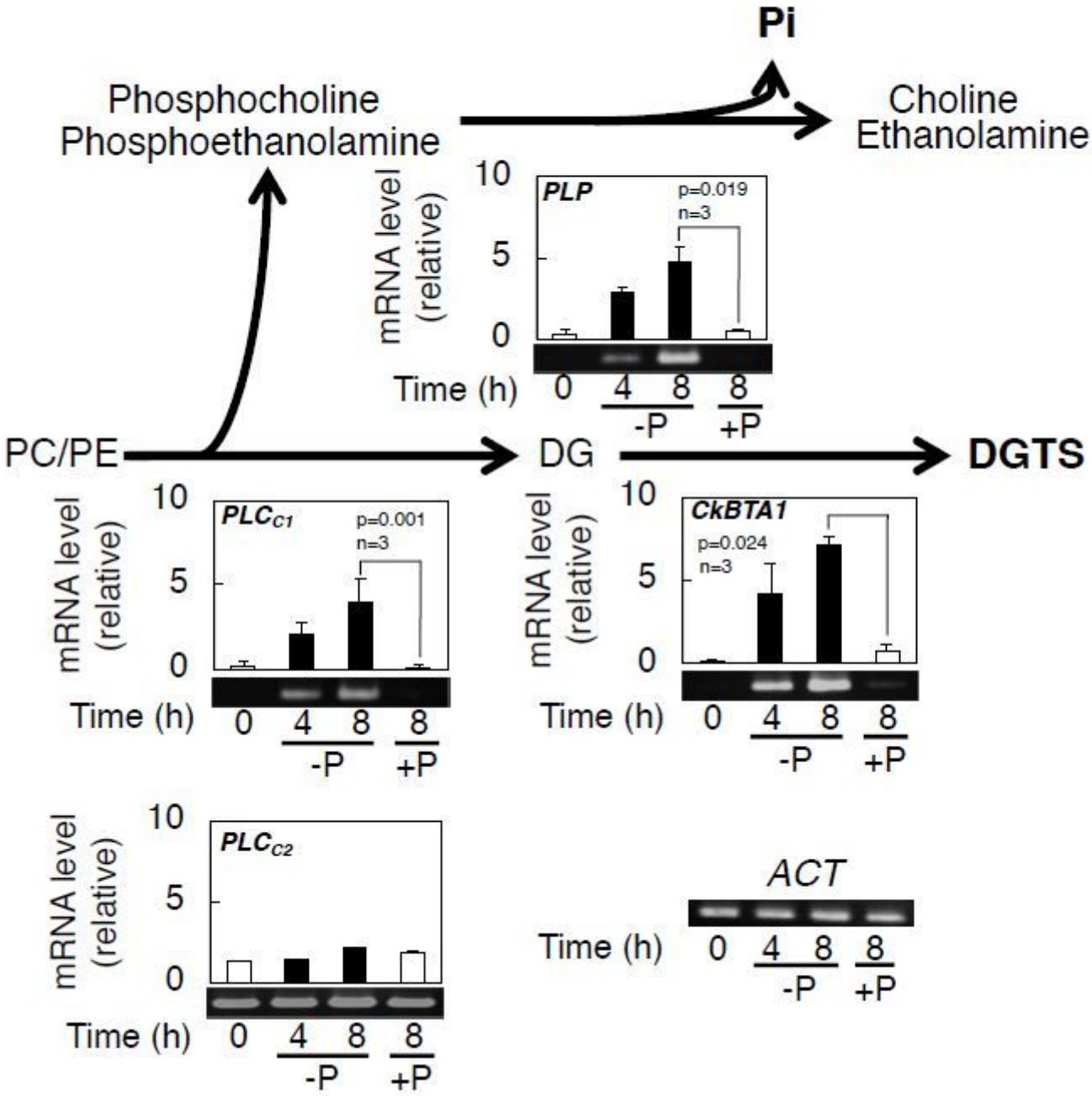

Figure 9

Regulatory expression of the genes for -P induced lipid remodeling in C. kessleri. The expression levels of the BTA1, PLCC1, PLCC2, and PLP genes were investigated through semi-quantitative RT-PCR analysis in C. kessleri cells before and after a shift to -P conditions. The intensities of the DNA bands that correspond to mRNAs of the individual genes were used for determination of the values, relative to that of ACT. The values shown are averages ± SEM for three biological replicates. Data were analyzed by one-tailed Student's t-test.

Supplementary Files

This is a list of supplementary files associated with this preprint. Click to download.

- s1.jpg
- supptables.docx